View metadata, citation and similar papers at core.ac.uk
brought to you by CORE
provided by Texas A&M University

SENSITIVITY ANALYSIS OF MODELING PARAMETERS THAT AFFECT THE DUAL PEAKING BEHAVIOR IN COALBED METHANE RESERVOIRS

A Thesis

by

AMARACHUKWU NGOZI OKEKE

Submitted to the Office of Graduate Studies of
Texas A&M University
in partial fulfillment of the requirements for the degree of

MASTER OF SCIENCE

August 2005

Major Subject: Petroleum Engineering

SENSITIVITY ANALYSIS OF MODELING PARAMETERS THAT AFFECT THE DUAL PEAKING BEHAVIOR IN COALBED METHANE RESERVOIRS

A Thesis

by

AMARACHUKWU NGOZI OKEKE

Submitted to the Office of Graduate Studies of
Texas A&M University
in partial fulfillment of the requirements for the degree of

MASTER OF SCIENCE

Approved by:

Chair of Committee,	Robert A. Wattenbarger
Committee Members,	Robert R. Berg
	James B. Maggard
Head of Department,	Stephen A. Holditch

August 2005

Major Subject: Petroleum Engineering

ABSTRACT

Sensitivity Analysis of Modeling Parameters That Affect the Dual Peaking Behavior in Coalbed Methane Reservoirs. (August 2005)

Amarachukwu Ngozi Okeke, B.Eng., Federal University of Technology. Owerri, Nigeria

Chair of Advisory Committee: Dr. Robert A. Wattenbarger

Coalbed methane reservoir (CBM) performance is controlled by a complex set of reservoir, geologic, completion and operational parameters and the inter-relationships between those parameters. Therefore in order to understand and analyze CBM prospects, it is necessary to understand the following; (1) the relative importance of each parameter, (2) how they change under different constraints, and (3) what they mean as input parameters to the simulator. CBM exhibits a number of obvious differences from conventional gas reservoirs, one of which is in its modeling.

This thesis includes a sensitivity study that provides a fuller understanding of the parameters involved in coalbed methane production, how coalbed methane reservoirs are modeled and the effects of the various modeling parameters on its reservoir performance. A dual porosity coalbed methane simulator is used to model primary production from a single well coal seam, for a variety of coal properties for this work. Varying different coal properties such as desorption time (τ), initial gas adsorbed (V_i), fracture and matrix permabilities (k_f and k_m), fracture and matrix porosity (ϕ_f and ϕ_m), initial fracture and matrix pressure (to enable modeling of saturated and undersaturated reservoirs), we have approximated different types of coals.

As part of the work, I will also investigate the modeling parameters that affect the dual peaking behavior observed during production from coalbed methane reservoirs. Generalized correlations, for a 2-D dimensional single well model are developed. The predictive equations can be used to predict the magnitude and time of peak gas rate.

DEDICATION

This work is dedicated to God and my wonderful mother, Florence, whose undoubting faith, encouragement and unfailing support saw me through and helped me achieve this goal.

ACKNOWLEDGEMENTS

I wish to express my sincere appreciation to the following for their contribution to this study:

Dr. Robert A. Wattenbarger, Professor of Petroleum Engineering, who served as a Chair of my committee, for his endless support, constant guidance and assistance throughout the course of this work. I feel most honored to have worked under his supervision.

Dr. James B. Maggard and Robert Berg for serving as members of my committee, and Mrs. Marylena Olave, Master of Science candidate, for helpful technical and moral support.

TABLE OF CONTENTS

Page

ABSTRACT……..iii

DEDICATION……..v

ACKNOWLEDGEMENTS……..vi

TABLE OF CONTENTS……...……..vii

LIST OF TABLES…….ix

LIST OF FIGURES…….. xi

CHAPTER

I INTRODUCTION……...1

1.1 Background…….…….…1
1.2 Objectives…….....2
1.3 Problem Description…….…….....3

II LITERATURE REVIEW ……..…….5

2.1 Coalbed Methane Gas Transport…….....5
2.2 Reservoir Models …….……..... ..5
2.3 Sensitivity Analysis on Modeling Parameters…….....……8
2.4 Dual Peaking Phenomena…….…….....9

III COALBED METHANE RESERVOIR MECHANICS…….....10

3.1 Gas Storage and Adsorption…….…….....10
3.2 Gas Transport Mechanism…….....11
3.3 Langmuir Theory…….…..14

IV NUMERICAL RESERVOIR MODEL …….....18

4.1 Dual Porosity Model…….…….…18
4.2 Description of CMG Simulator…….…….…19
4.2.1 Dual Porosity Formulations in CMG…….……....20
4.2.2 Adsorption and Diffusion ...…….21

V SENSITIVITY ANALYSIS AND DISCUSSION…….…….…..25

CHAPTER Page

5.1 2 Dimensional Single Well Model…….…….25
5.2 Sensitivity Analysis…….….....28
5.3 Effects of Coal Seam Modeling Parameters on Gas Rates…..…29
5.3.1 DesorptionTime……....30
5.3.2 Matrix Permeability……..32
5.3.3 Fracture System Permeability……...33
5.3.4 Coal Matrix Porosity, $\varnothing_m$…….....35
5.3.5 Fracture System Porosity, $\varnothing_f$……....37
5.3.6 Initially Adsorbed Gas…….….39
5.3.7 Saturated and Undersaturated Coalbed Methane Reservoirs……..41
5.4 Investigating the Dual Peaking Behavior…….…44

VI GENERALIZED CORRELATIONS …….. ……...47

6.1 Dual Peaking…….……..……..…47
6.2 Simulations Base Case…….……...50
6.3 Generalized Correlations…….……....50
6.3.1 Simple Linear Regression…….…….…..…51
6.3.2 Multiple Regression……..……...…..……..….52

VII CONCLUSIONS AND RECOMMENDATIONS…….....61

7.1 Sensitivity Analysis…… …..61
7.2 Generalized Correlations …….……..…62
7.3 Recommendations for Future Work…….……..…63

NOMENCLATURE…….....64

REFERENCES…….…… …66

APPENDIX A CMG BASE CASE DATA FILE…… … ….69

APPENDIX B DESORPTION TIME AND RATE EQUATIONS FOR COALBED METHANE…….……..…..76

APPENDIX C CORRELATION DATA AND REGRESSIONAL ANALYSIS PLOTS……...….80

APPENDIX D DESCRIPTION OF THE EFFECT OF FRACTURE AND MATRIX PRESSURES ON GAS RATES…….92

Page

VITA…….. …...94

LIST OF TABLES

TABLE Page

4.1 Differences between the Warren and Root model and Coalbed Methane……... 19

5.1 Base case coal reservoir properties ……..……27

5.2 Data range for input modeling parameter for sensitivity analysis……..…. .30

5.3 Effect of variation in coal matrix porosity on the adsorbed gas and surface gas volumes …….……..... 37

6.1 Simple linear regression equations…….……..51

C-1 Correlation sample data…… ….…...80

C-2 Simulation cases…….…. .91

LIST OF FIGURES

FIGURE Page

3.1 Illustration of the large internal surface area possessed by coal particles……...11

3.2 Schematic of methane transport in a coal seam (After Remner[2])…….. 14

3.3 Example of a sorption isotherm, which defines the holding capacity of gas as a function of pressure……..16

3.4 Production history of a coalbed methane well…… 17

4.1 Dual porosity model…… …... 20

5.1 21*21 Simulation model grid model……..... 26

5.2 Gas and water relative permeability curve……..… 28

5.3 Effect of desorption time on gas for varying only the desorption time (τ)…… 31

5.4 Effect of desorption time water rate for varying only the desorption time (τ)……..…….……. 32

5.5 Simulation results showing that varying the matrix permeability does not affect the gas rate……..…….…….. 33

5.6 Simulation results show that gas production rate increases with increase in the permeability……...……..... 34

5.7 Simulation results show that water production rate increases with increase in the permeability……..…….…….. 34

5.8 Simulation results show that gas production rate increases with the matrix porosity. …….…….. 36

5.9 Simulation results show that water production rate is not sensitive to change in the matrix porosity, …….…….. 36

FIGURE Page

5.10 Simulated gas production for variation in the fracture porosity shows increase in the production rate with decrease in porosity…… …..38

5.11 Simulated water production rates, shows significant effect of variations in the fracture porosity…… ….38

5.12 Simulation results show the first peak becoming more evident as the matrix gas content increases and the second peak diminishes. …… …...40

5.13 Simulation results show the low gas content coals with higher water rates as expected…… …….....40

5.14 Simulation results show the gas rates and the effect of reservoir type; saturated or undersaturated of various V_i (initial gas adsorbed volume) values…….....……. 42

5.15 Simulation results show corresponding higher water rates for undersaturated cases when compared to the saturated cases for various V_i (initial gas adsorbed volume) values…… …….……43

5.16 Simulation results show the effect of reservoir type; saturated or undersaturated on the desorption time ……43

5.17 Simulation results show corresponding higher water rates for undersaturated cases when compared to the saturated cases for various desorption time, τ values ……..……..…… ... .44

5.18 Simulation results for gas production from a typical dual peaking case of V_i =2.5 scf/day and τ = 10 days……..…… . .45

5.19 Gas saturation profile, showing that the 1st peak occurs before fracture

FIGURE Page

pressure in the boundary grid blocks are depressurized to the matrix pressure. And the 2nd peak occurs after the boundary effect…… ..…46

6.1 Simulated CBM gas production showing the double peaks of gas rates… …... 48

6.2 Simulated CBM water production rates showing a continuous decline in the water rates after the 1st peak…….… ……..……...49

6.2 Impact of permeability anisotropy on gas flow rate, shows that for an isotropic square drainage area there is no dual peaking[22]…….…….. 49

6.4a Generalized correlation for t_1……..…..55

6.4b Generalized correlation for t_1 for increased gas rates……..…….55

6.5 New points generated from simulation results to test the correlation equation for t_1. …….. .. 56

6.6 Generalized correlation for t_2……57

6.7 New points to test the correlation equation for t_2……...…….. .. 58

6.8 Generalized correlation for q_1…….… .59

6.9 New points to test the correlation equation for q_1…… .. 59

6.10 Generalized correlation for q_2…… …..60

6.11 New points to test the correlation equation for q_2…… 60

C-1 Simple regression analysis plot showing the linear relationship between t_1 and the initially adsorbed gas volume, V_i 82

C-2 Simple regression analysis plot showing the linear relationship between t_2 and the initially adsorbed gas volume, V_i...…….. 83

C-3 Simple regression analysis plot showing the linear relationship between q_1

FIGURE Page

and the initially adsorbed gas volume, V_i 83

C-4 Simple regression analysis plot showing the linear relationship between q_2 and the initially adsorbed gas volume, V_i 84

C-5 Simple regression analysis plot showing the linear relationship between t_1 and the desorption time, τ 84

C-6 Simple regression analysis plot showing the linear relationship between t_2 and the desorption time, τ 85

C-7 Simple regression analysis plot showing the linear relationship between q_1 and the desorption time, τ 85

C-8 regression analysis plot showing the linear relationship between q_2 and the desorption time, τ 86

C-9 Simple regression analysis plot showing the linear relationship between t_1 and the fracture porosity, $\varnothing_f$ 86

C-10 Simple regression analysis plot showing the linear relationship between t_2 and the fracture porosity, $\varnothing_f$ 87

C-11 Simple regression analysis plot showing the linear relationship between q_1 and the fracture porosity, $\varnothing_f$ 87

C-12 Simple regression analysis plot showing the linear relationship between q_2 and the fracture porosity, $\varnothing_f$ 88

C-13 Simple regression analysis plot showing the linear relationship between t_1 and the matrix porosity, $\varnothing_m$ 88

C-14 Simple regression analysis plot showing the linear relationship

FIGURE Page

between t_2 and matrix porosity, $\varnothing_m$ ……. 89

C-15 Simple regression analysis plot showing the linear relationship between q_1 and matrix porosity, $\varnothing_m$ ……..……..89

C-16 Simple regression analysis plot showing the linear relationship between q_2 and matrix porosity, $\varnothing_m$.....…90

D-1 Change in the matrix and fracture pressures with time for the varying cases of V_i ranging from 2.27E-10 scf/ft^3 to 3735 scf/ft^3……....…93

CHAPTER I

INTRODUCTION

1.1 Background

Coalbed methane was merely an environmental safety issue and enemy to the coal producer because of the apparent danger and cost to underground mining. So coalbed methane wells were initially drilled to release gas as safety measures for coal mining operations.

Increase in gas prices in the late 70's catalyzed the merging of technology and market forces to transform this former waste product to a valuable resource. 2003 Energy Information Administration (EIA) statistics showed that coalbed methane contributes to about 10% of U.S proven reserves of natural gas which is estimated to be about 18,743 Bcf and 8% of U.S. gas production estimated at 1,600 Bcf *.

As a coal formed from organic matter matures, several gases, including carbon monoxide and methane are produced. During this process of coal formation (coalification), large quantities of gas is generated and stored on the internal surfaces of the coal. Because of the extensive internal surface area possessed by coals, it is able to store large amounts of methane; 6 to 7 times more than a conventional gas reservoir of equal rock volume can hold. Due to this characteristic, production wells are drilled and perforated directly into the coal seam to produce the gas (methane).

This thesis follows the style of the *Journal of Petroleum Technology.*
*Information from www.usgs.gov

Understanding of the geology and production of coalbed methane is still in its early learning years and much is to be learned about the occurrence and recoverability of this resource which is essentially the contribution this work brings.

1.2 Objectives

The overall goal of this work is to illustrate and document fundamental modeling techniques for coalbed methane reservoirs while also studying the effects of a variety of coal properties on primary production from a coal seam. As part of the work using reservoir simulation, sensitivity analysis is conducted on various modeling parameters to determine how each parameter would most affect gas flow and modeling of a coalbed methane reservoir.

In the field, a unique behavior called "dual peaking" has been observed and this feature was also observed in simulation results in the course of this work. Simulation results indicated a "dual peak" behavior when certain modeling parameters were varied beyond a certain range. This study analyzes the occurrence of this feature and the modeling parameters that affect it.

Additionally, using the Addington[1] method of correlation, a generalized correlation is developed to predict the magnitude (q_1 and q_2) and time to peak (t_1 and t_2) gas rate. This method of correlation utilizes data from simulation results for a specific model and within a given range of data, to make predictions based on individual well modeling parameters.

1.3 Problem Description

Prior studies have considered the effect of coal seam properties on methane production. Remner et al [2] in their work developed a mathematical model that simulated the flow of methane and water through a coal seam and investigated the effect of coal seam properties on gas drainage for single and multiple well systems. Also, other authors such as Odusote et al. [3] investigated the effects of coal seam properties on gas flow for enhanced coalbed methane production as determined from numerical simulation. Their results showed the various properties most likely to affect methane recovery. However, none of these wide ranges of work on different subjects in coalbed methane simulation illustrates and documents the fundamental numerical modeling techniques for coalbed methane such that an engineer new to this unique modeling of coalbed methane reservoirs can have a source of reference.

Field production data has been seen to exhibit a double peaking behavior in gas rates. This feature is referred to as “dual peaking”. The dual peaking gas rate behavior was also observed in numerical simulation results and this lead to this study, which will investigate the modeling parameters that controlled this unique behavior.

Chaianansutcharit, et al[4] analyzed the occurrence of the unique “dual peak” as a feature that can be used to diagnose permeability anisotropy and infer drainage shape by considering the impact of permeability anisotropy and pressure interference on coalbed methane. Their work showed that the permeability anisotropy and drainage area were the major factors that determined if the dual peak gas behavior will be seen; details will be

discussed in the literature review. Additionally, this work will show the effect of modeling parameters on the dual peaking feature.

CHAPTER II

LITERATURE REVIEW

2.1 Coalbed Methane Gas Transport

Cervik in 1967[5], presents the fundamental concepts governing the transport of gas in an adsorbed or free gas state through a coal seam. The work stated that the desorption of gas depends upon equilibrated pressure, coal particles size, geometry and diffusivity coefficient, such that smaller particles would release more gas. They classified coalbeds into 3 categories according to their modes of transport: 1) predominately Fick's law, 2) combination of Fick's and Darcy's law, and 3) predominately Darcy's law. They finally concluded that the extension of the conventional methods of reservoir engineering analysis to coalbeds will not be justified since the mass transport in this system is governed by Darcy's and Fick's law.

2.2 Reservoir Models

The dual porosity reservoir system in coalbeds is similar to that proposed by Warren and Root [6] in 1962. They were the first to develop an idealized model for studying the characteristic behavior of a permeable medium which contains regions that significantly contributed to the pore volume, but negligible to the flow capacity of the system. Example of such a medium is a naturally fractured reservoir such as coalbed methane reservoir. They described two classes of porosity namely; primary porosity (controlled by deposition and lithification), and secondary porosity (controlled by fracturing, jointing and solution in water). An unsteady state flow of this idealized model reservoir was

described mathematically and pressure build-up performance examined to suggest a technique for analyzing the build-up data to evaluate these two necessary parameters. They concluded the parameters ω and λ are sufficient to characterize the behavior of a dual porosity system. ω is a measure of the fluid capacitance of the secondary porosity and the λ is related to the scale of heterogeneity that is present in the system.

In 2001, Reeves and Pekot[7] presented a model for desorption controlled reservoir called the triple-porosity/dual permeability model, a modification of the Warren and Root[6] model. They stated that the widely accepted historical dual porosity/single permeability model approach for coals has shown errors when forecasting well or field performance. These errors include the overestimation of gas production being and under estimation of water production, and also inconsistency with field data. Gas production, in practice, occurred much later than these models predicted; therefore so an additional porosity and permeability system is required to account for this effect. A third porosity was incorporated in the matrix block to provide needed free gas (and water) storage capacity for material balance. This also allows for the desorption from the matrix and diffusion through the micro-permeability matrix into the cleat system to be decoupled and modeled explicitly. "Comparison of this new model and historical modeling approach showed that new model predicted lower gas and higher water production rates" which matched field results. A new coalbed methane simulator, COMET2 was developed based on these modifications.

The use of conventional reservoir simulators for modeling coalbed methane reservoirs was described in 1990 by Seidle[8]. They showed that if the rate of diffusion of gas from the matrix is rapid compared to the rate of flow of gas and water through in the cleats; then it could be assumed that the desorption process is instantaneous. This assumption will therefore allow the adsorption of gas to the coal surface to be modeled as gas dissolved in immobile oil, thereby making the use of conventional reservoir simulators possible. Modifications to the porosity and gas and water relative permeability to account for the pseudo oil are required. Comparative results between the black oil simulator and COMETPC (a coalbed methane simulator developed by ICF-Lewin) showed qualitative agreement. A notable difference in the simulators was seen in prediction of peak gas rate and time. They suspected that this could be a result of time dependent gas desorption in COMETPC compared to infinite desorption in the conventional black oil simulator.

In 2002, Tan[9], using the approach presented by Seidle[8] presented an independent implementation into a commercial conventional reservoir simulator. They compared their results with that of Seidle and Paul[10]. To demonstrate the delayed effect in gas production, they investigated the effects of pressure dependent permeability and porosity on producing water and gas rates by making a series of comparative runs. Comparison of results with those published by Seidle unfortunately did not show a good match, but when compared with those of Paul, excellent agreement was reported. They also concluded that the dual grid approach for matrix fracture simulation provides more accuracy for coal matrix-cleats modeling. To overcome some of the inherent difficulties generated by coalbed methane models presented in early papers in 2003, Guo[11] presented

a new 3 dimensional, two-phase flow coalbed-methane (CBM) numerical simulator. The new model permits the description of the phenomena occurring within the fractures and the coal micropores, which enhances our understanding of the coalbed production behavior. In this new model, the volume of gas released from the coal can be predicted by a sorption isotherm from experiments or calculations, so whether it is equilibrium or non-equilibrium sorption is irrelevant.

2.3 Sensitivity Analysis on Modeling Parameters

Sensitivity analysis and parametric studies have been addressed by authors like Remner, et al [2] to investigate the effects of reservoir properties on gas drainage efficiency for a single well system. Their work showed that the magnitude of the early desorption peak was a function of the ability of the matrix to supply its adsorbed gas to the fracture and coal seams conductivity to water.

Odusote, et al[3] specifically focused on the effect of coal seam properties on enhanced coalbed methane (ECBM) production. Based on reservoir simulation results, they showed that certain reservoir parameters like permeability, coal density, Langmuir volume etc are most likely to affect methane recovery and CO_2 sequestration.

Derickson, et al[12] as part of their work to evaluate the Huaibei area for coalbed methane production, evaluated the sensitivity of fundamental coal properties (such as permeability, porosity, gas content, gas saturation and coal thickness) to production rates

and ultimate recovery. They concluded that this sensitivity of coal modeling properties will be an important tool in future decision making.

2.4 Dual Peaking Phenomena

Chaianansutcharit, et al[4] analyzed the impact of permeability anisotropy and pressure interference on coalbed methane performance. Their study described the occurrence of the unique "dual peak" as a feature that can be used to diagnose permeability anisotropy and infer drainage shape by considering the impact of permeability anisotropy and pressure interference on coalbed methane. They identified that the unique behavior is caused by the different timing of boundary effects such as can be seen in anisotropic permeability in a square area and isotropic permeability in a rectangular area. Their worked showed that the permeability anisotropy and drainage area were the major factors that determined if the dual peak gas behavior will be seen. This work investigates other parameters for which this "dual peaking" is sensitive even for isotopic permeability in a rectangular area.

Using the Addington[1] method of correlation, a generalized correlation is developed to predict the time to peak (1st and 2nd) and the peak gas rate (magnitude). This correlation method utilizes data from simulation results for a specific model and within a given range of data to make predictions based on individual well modeling parameters and production rate.

CHAPTER III

COALBED METHANE RESERVOIR MECHANICS

3.1 Gas Storage and Adsorption

Coalbed methane is natural gas or methane (CH_4) that occurs in coalbeds and is formed during the conversion of plant material to coal; a process called coalification. Because coalbeds serve as both the source rocks and reservoir rocks, they have been found to be considerably different from normal porous gas reservoirs in both their storage and flow characteristics. Gas is held in coal in four possible ways: 1) as free gas within the micropores (are pores with a diameter of less than 0.0025 inches), 2) as adsorbed methane molecules on the surface of micropores held by molecular attraction, 3) as free gas within fractures or pores, and 4) as dissolved gas in formation water. It is important to note that 98% of gas within a coal seam is stored by adsorption. Also, this physical adsorbtion between methane and the coal solid molecules involves intermolecular forces (Van der Waals forces).

Coalbed methane is an attractive prospect for development because of their ability to retain a higher amount of gas at shallow depths in comparison to conventional reservoirs of equivalent depth and pressure. The large internal surface area possessed by coal contributes to making this resource very viable, since it is able to store large amounts of methane. Coals are able to store large amounts of methane; 6 to 7 times more than a conventional gas reservoir of equal rock volume can hold.

Marsh[5] reviewed various methods of determining surface area of coal and concluded that the surface area of coals is mostly in the range of 2150 – 3150 ft^2/g. This also means that if a micro-particle of coal is crushed its surface area can be a large as a 296 ft X 147 ft football field. This is illustrated in **Figure 3.1**.

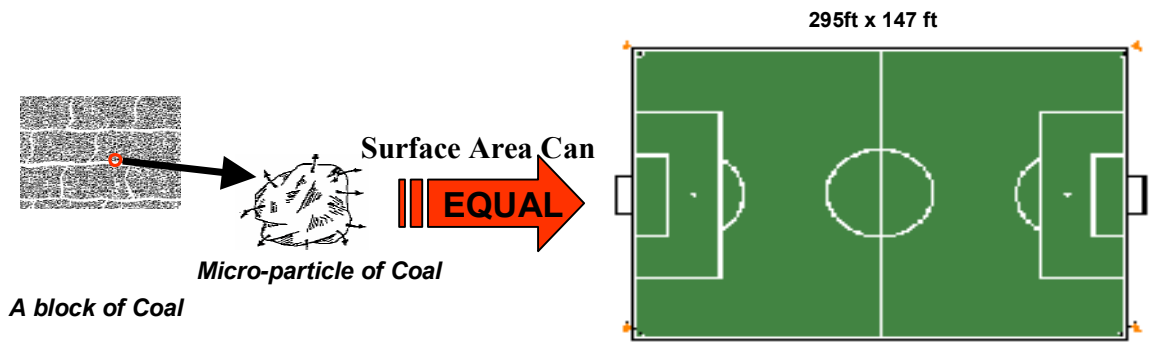

Figure 3.1- Illustration of the large internal surface area possessed by coal particles.

3.2 Gas Transport Mechanism

Coalbed reservoirs consist of two important elements the matrix (micro-pore system) and the fractures (macro-pore system). And each of these elements has its distinct method of transporting gas as is illustrated in the Figure on page 14.

Gas flow in coals is in two phases; first the gas desorbs from the matrix and diffuses into the natural fractures, secondly gas flows via the fracture/cleats to the production well. Gas transport through the matrix (primary porosity system) is a diffusion process and a concentration gradient is the driving force for the flow and it is quantified with Fick's law[13]:

$$q_g = -DA\frac{\partial C}{\partial L} \quad \text{.....3.1}$$

While the water and gas flow (two phase flow) to the well bore via the cleat system (secondary porosity system) has a pressure gradient as the driving force and obeys Darcy's law[11]:

$$q_g = -\frac{k_g A}{\mu_g}\frac{\partial p}{\partial L} \quad \text{.....3.2}$$

Although the two transportation phenomena are separate and distinct, they are interdependent. Jochen[14] shows the equations that describe water and gas flow in coalbed methane reservoirs, and are also solved in the reservoir simulator as the following:

The macro-pore water transport equation is

$$\frac{1}{r}\frac{\partial}{\partial r}\left[\frac{K_w}{\mu_w B_w} r \frac{\partial p_w}{\partial r}\right] = \frac{\partial}{\partial t}\left[\phi \frac{S_w}{B_w}\right] \quad \text{.....3.3}$$

The macro-pore gas transport equation is

$$\frac{1}{r}\frac{\partial}{\partial r}\left[\frac{K_g}{\mu_g B_g} r \frac{\partial p_g}{\partial r}\right] + q = \frac{\partial}{\partial t}\left[\phi \frac{S_g}{B_g}\right] \quad \text{.....3.4}$$

Where,

$$q = -F_g \frac{\partial C}{\partial t} \quad \text{.....3.5}$$

And q represents the desorption/diffusion source term for pseudosteady state diffusion and F_g is a dimensionless geometric shape factor for various micro-pore matrix geometries.

The diffusion of gas out of the coal matrix can be expressed by a simple diffusion equation:

$$\frac{\partial C}{\partial t} = DF_s[\overline{C} - C(p_f)] \quad \text{.....3.6}$$

Where $\overline{C}$ is the average gas concentration in the coal matrix and $C(p_f)$ is the gas concentration in the fracture at the fracture pressure. $\overline{C}$ is the average gas concentration in the matrix calculated by time step by time step material balance on a time step by step Combining Eqn. 3.5 and Eqn. 3.6, the equation for the diffusion/desorption term becomes

$$q = -F_g DF_s[\overline{C} - C(p_f)] \quad \text{.....3.7}$$

Where F_s is the primary porosity shape factor. The product $F_g DF_s$ is often written as $\frac{1}{\tau}$, where τ is the pseudo steady state diffusion time constant, also referred to as the desorption time and is defined as

$$\tau = \frac{1}{F_g DF_s} \quad \text{.....3.8}$$

And Eqn 3.7, the diffusion/desorption term becomes

$$q = -\frac{1}{\tau}\left[\overline{C} - C(p_f)\right] \quad \text{.....3.9}$$

The desorption time (τ) takes into account the amount of time required for the gas to desorb from coal matrix and diffuses to the fractures. Although diffusivity values are normally used in reservoir models, an easier way of representing this same concept is in terms of the desorption time. Desorption time is also defined as the time required to desorb 63.2% of the original gas content if a sample is maintained at constant temperature[15], see Appendix B for details. The desorption time is determined from a laboratory experiment called canister test. During this test, core samples are collected and

sealed in desorption canisters and equilibrated to approximate reservoir temperature after which volume of desorbed gas is measured with time.

Remner[2] shows that the sorption time constant can be expressed as:

$$\tau = \frac{R_i^{\,2}}{(D)} \quad \ldots\ldots\ldots\ldots\ldots\ldots\ldots\ldots\ldots\ldots\ldots\ldots\ldots\ldots\ldots\ldots\ldots\ldots\ldots\ldots\ldots\ldots 3.10$$

Where D is the diffusivity coefficient, ft^2/day and R_i is the radius of spherical micropore sub element, ft.

A schematic illustrating the fluid transport in coal is shown in **Figure 3.2**.

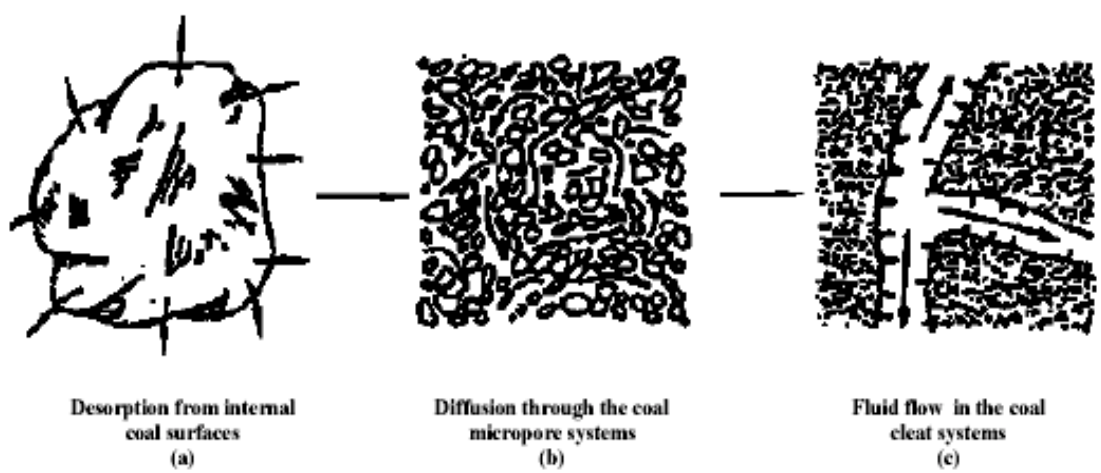

Figure 3.2- Schematic of methane transport in a coal seam (After Remner[2]).

3.3 Langmuir Theory

The Langmuir isotherm was developed by Irving Langmuir in 1916 to describe the dependence of the surface coverage of an adsorbed gas on the pressure of the gas above the surface at a fixed temperature[16].

Kohler and Ertekin[17] has shown that gas storage is dependent on the sorption isotherm and adsorption typically is modeled with an adsorption isotherm[13]. For unconventional reservoirs, the most commonly used isotherm is the Langmuir isotherm. The Langmuir isotherm is based on the theory that simply states that the rate of molecules arriving and adsorbing on the solid surface should equal the rate of molecules leaving the solid surface. Whenever a gas is in contact with a solid, there will be an equilibrium established between the molecules in the gas phase and the corresponding adsorbed species (molecules or atoms) which are bound to the surface of the solid[16]. The isotherm is used to predict the release of gas from the reservoir as the pressure is reduced to the desorption pressure. A coal sorption isotherm is an important laboratory analysis that shows the relationship between the gas content of a coal and its maximum gas storage capacity. **Figure 3.3,** shows a typical sorption isotherm used to describe the amount of gas sorbed per unit with pressure variations.

The relationship used to represent the sorption mechanism in coalbed methane reservoirs is the Langmuir's equation:

$$V(p) = V_L \frac{p}{p + p_L} \quad \text{.....} \quad 3.11$$

Where V is the gas content at p in scf/ft^3, and V_L is the Langmuir Volume in scf/ft^3, p_L is the Langmuir pressure in psi and p is the gas pressure in psi. In the above equation, the Langmuir volume is the saturated monolayer volume while the Langmuir pressure is the pressure at half of the Langmuir volume. The concentration described in the above equation is in equilibrium with the surrounding free gas at pressure p.

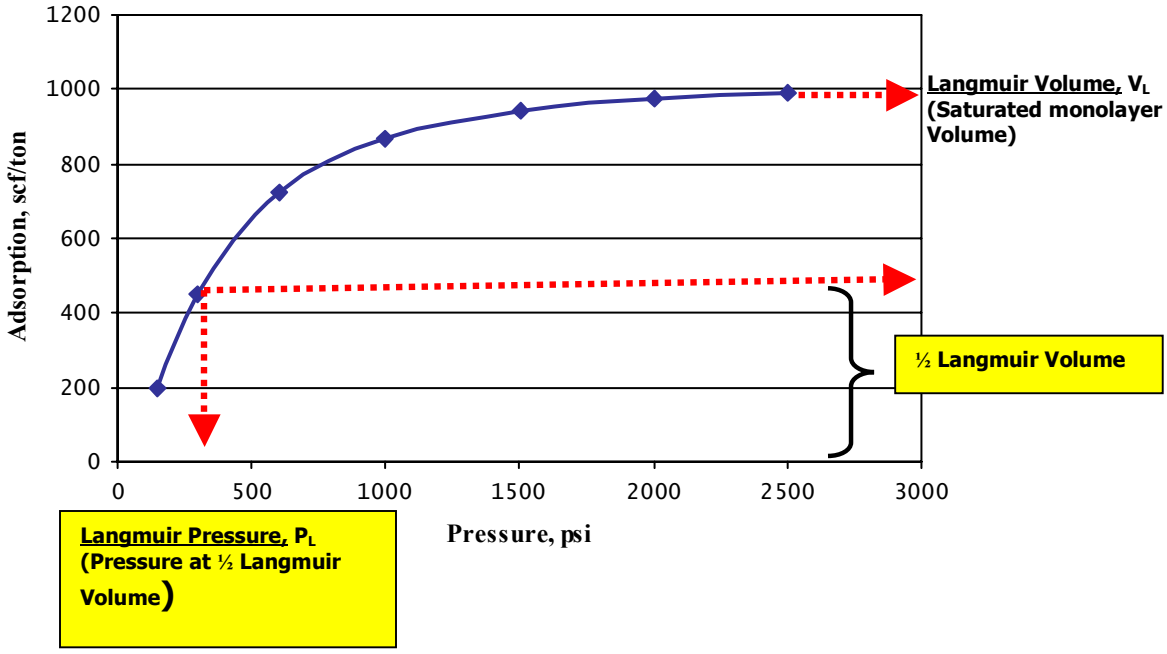

Figure 3.3- Example of a sorption isotherm, which defines the holding capacity of gas as a function of pressure.

Since pressure reduction frees the methane molecules from the coal and allows gas migration. Therefore, in order to produce gas from the coal, the adsorbed gas must first be desorbed from the coal and this is accomplished by depressurizing the coal to the "critical desorption pressure" the coal. This depressurization is accomplished through the production of the formation water, which exists in the natural fracture system. As the water is withdrawn and formation pressure declines, the produced gas volumes tend to build from a low initial rate to a maximum rate after several years. This is a direct contrast with conventional reservoirs where the highest production rates are at the beginning of production and this decline with the years, see **Figure 3.4.**

So, when the initial reservoir pressure is above the critical desorption pressure, the reservoir is called an under-saturated reservoir. As the gas saturation increases in the fracture gas flows from the matrix to the fracture, the k_{rg} increases until the critical saturation is reached when the reservoir starts producing gas with water.

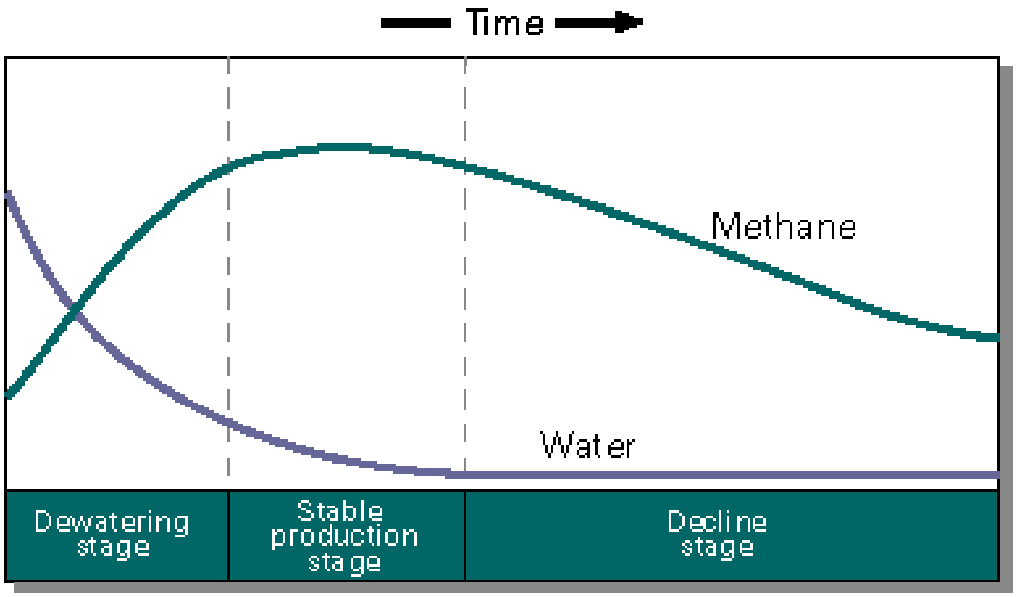

Figure 3.4- Production history of a coalbed methane well. Modified from U.S. Geological Survey, Energy Resource Surveys Program, 1999, Coalbed Methane – an untapped energy resource and an environmental concern: U.S Geological Survey web site on coalbed methane.

CHAPTER IV

NUMERICAL RESERVOIR MODEL

4.1 Dual Porosity Model

Naturally fractured reservoir performance can be modeled using the dual porosity model, which defines porosity and permeability one for the matrix block and the other for the fracture block. This model assumes that flow is from the matrix block to the fracture block.

Warren and Root[6] in 1963 developed an idealized model for studying the behavior of a permeable formation, which has regions that contribute to the pore volume but negligible to flow. Examples of reservoirs that this model, could represent include naturally fractured reservoirs.

A modified Warren and Root dual porosity model accounts for the diffusive flow of the adsorbed gas from the matrix to the fracture. This is used to describe the physical processes involved in a typical coalbed seam, which is representative of the coal/cleat system. The dual porosity model consists of two dependent and interconnected systems representing the matrix and the permeable rock fractures.

A difference between the dual porosity model and coalbed methane models is that

unlike in the dual porosity oil reservoir model, where the matrix pressure and oil saturation is tracked in the coalbed methane only the gas concentration is tracked. Another difference is in initial gas storage and matrix/fracture flow are shown in Table 4.1.

Table 4.1- Differences between the Warren and Root model and coalbed methane reservoirs

	Warren & Root	**Coalbed Methane**
Initial Gas Storage	*Free gas in pores OR Fractures (Cleats)*	*Adsorbed to coal OR Free gas in fractures*
Matrix / fracture flow	**"Pseudo Steady State Model"** $\hat{q} = C(p_m - p_f)$	$q = \frac{1}{\tau}\left[\overline{C} - C(p_f)\right]$
	Darcy's Law	*Fick's Law (Diffusion)*

4.2 Description of CMG Simulator

CMG, a two-phase compositional coalbed methane reservoir simulator is used for the modeling. The numerical formulations and solution protocols on which this model is based can be found in the GEM 2003.10 users guide.

GEM 2003.10 is a compositional simulator capable of modeling both missed gas diffusion and non-instantaneous diffusion rates. It comes incorporated as part of the

Computer Modeling Group's (CMG's) package of simulation tools. In GEM the coalbed methane model is built using the dual porosity option (DUAL POR) and the sorption isotherms are modeled after the Langmuir's Sorption isotherm. The flow in the fractures will consist of gas/water simulated using the standard Darcy model. The simulator disables all matrix-to-fracture Darcy flow when coalbed modeling is used, since the assumption is that the flow is a diffusive process. This inherently makes the matrix permeability redundant, a small positive value is input to indicate a pathway for diffusion to occur between matrix (coal) and fracture (cleat)[18].

For modeling the rock properties two relative permeability tables are defined for the matrix and fracture flow, but since there is no Darcy flow modeled from the matrix to the fracture, the relative permeability table for the matrix is understood to be redundant.

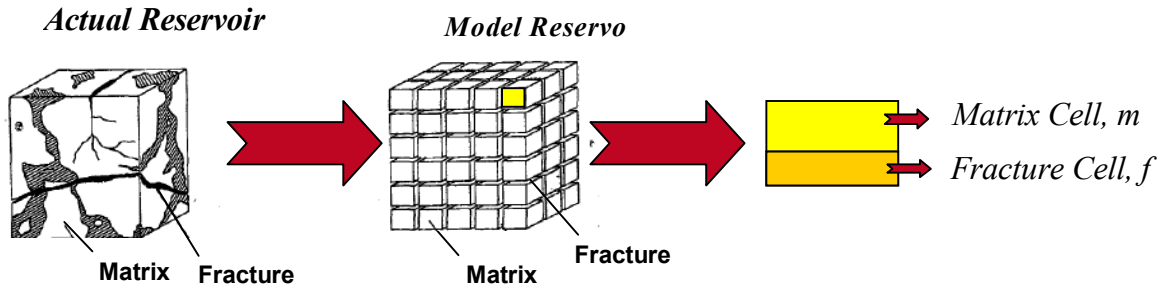

Figure 4.1- Dual porosity model.

4.2.1 Dual Porosity Formulations in CMG

The DUALPOR option in CMG allows each reservoir grid block to have up to two porosity systems; one for the matrix and the other for the fracture. Matrix properties are

denoted by the use of the *MATRIX keyword and fracture properties are denoted by the use of *FRACTURE keyword.

4.2.2 Adsorption and Diffusion

Selecting the LANG-DIFFUSION-COAL keyword indicates that the coal-cleat diffusion modeling will calculate the concentration gradients for the diffusive flow calculation based on the Langmuir adsorption data. The concentration of gas on the surface of the coal is assumed to be solely pressure dependent and this is described by the Langmuir isotherm.

This LANG-DIFFUSION-COAL model can be described by the following equation[19];

*q(Lang,k) = Vol * [Shape * Diffus(k)] * F(Sg) * (Lang(k,m)- Lang(k,f))*……..4.1

Where,

Lang(k,m) = Extended Langmuir isotherm for the coal, multiplied by coal density, evaluated at matrix composition and pressure.

Lang(k,f) = Extended Langmuir isotherm for the coal, multiplied by coal density, evaluated at fracture composition and pressure.

Also, CMG also gives its equivalent equation for gas flow reduce space as;

$$Rate_{Block} = Vol * Shape * Diffus(k) * S_g^{A-\mathrm{mod}} * (C(k, gas, m) - C(k, gas, f)) \qquad \ldots 4.2$$

Where,

Vol = Bulk Volume

Shape = Shape factor (matrix-fracture interface area per unit volume)

$$= \quad Shape = 4 * \sum \left(1 / FracSpacing)^2\right)$$

Diffus(k)= Diffusion value (COAL-DIF-COMP)

$Sg^{A\text{-}mod}$ = gas saturation in the matrix (default = 1)

C(k,gas,m) = Concentration of component 'k' in gas phase of matrix cell "m"

C(k,gas,f) = Concentration of component 'k' in gas phase of fracture cell "f"

C(k,gas,f) in Eqn 4.2**,** represents the surface gas concentration which is a function of fracture pressure given by the Langmuir isotherm. The Langmuir isotherm can be defined in two ways;

1) by inputting the maximum moles of adsorbed component per unit mass of rock (gmole of component/kg of rock/lb of rock) using the *ADSORBTMAX keyword and also inputting a keyword *ADSTAB followed by a two column table showing the amount of component 'component_name' adsorbing (gmole of component/kg of rock/lb of rock) as a function of partial pressure of that component.
2) by defining the isotherm curvature by inputting just the maximum concentration V_i, using the *ADGMAXC and the Langmuir pressure constant $1/p_L$, using the *ADGCSTC.

The overall mass transfer rate from matrix (coal) to fracture (cleats), which will include the flow within the matrix as well as the sorption / desorption flow is represented by a parameter called the desorption time τ. This value is closely related to the diffusion

coefficient and cleat spacing of the coal and is specified by the COAL-DIF-TIME key word. The COAL-DIF-TIME can be defined in the simulator as a single number as opposed to inputting a shape factor and a diffusion coefficient. This single number defines how fast the gas is desorbing and flowing out through the cleat system; therefore, for smaller values of τ , the mass transfer is rapid and equilibrium between the micro pores and fracture is more easily maintained. The equilibrium is not maintained when the desorption time becomes a sizeable fraction for the time of the process. The value of the time constant is approximated using the following equations in CMG;

$$\tau = \frac{1}{shape * Diffus(k)} \quad \ldots\ldots\ldots\ldots\ldots\ldots\ldots\ldots\ldots\ldots\ldots\ldots\ldots\ldots\ldots\ldots\ldots\ldots 4.3$$

$$shape = 4 * \sum\left[\left(\frac{1}{DIFRAC^2}\right) + \left(\frac{1}{DJFRAC^2}\right) + \left(\frac{1}{DKFRAC^2}\right)\right] \ldots\ldots\ldots\ldots\ldots\ldots\ldots 4.4$$

Where *Diffus(K)* (cm^2/sec) represents the micro pores diffusion coefficient and the shape is the shape factor as proposed by Kazemi. *DIFRAC, DJFRAC, DKFRAC* refers to the set of fracture spacing.

CMG also has the option of inputting the diffusion coefficient instead of desorption time (COAL-DIF-TIME). This is specified by the COAL-DIF-COMP keyword.

The matrix made up of the solid coal and micro pores generally is modeled to have a higher porosity than the fractures but a much lower permeability, which makes the fracture the main conduit for flow in the system. 99% of the methane is in sorbed form on the surface of the coal. Fracture / cleats that permeate coalbeds are filled with water, so in

order to produce the gas (by desorbtion) the partial pressure of the gas must be reduced by producing the water (dewatering). During production, with an inherent pressure reduction in reservoir pressure the methane is desorbed from the coal and flows to the cleat system. This model represents the unsteady-state adsorption system where the amount of gas adsorbed is a function of both pressure and time.

Finite difference equation for dual porosity developed by Gilman and Kazemi[20] are used in CMG for modeling the conservation of oil and water in the fracture and matrix systems.

CHAPTER V

SENSITIVITY ANALYSIS AND DISCUSSION

5.1 2-Dimensional Single Well Model

Simulations of the base case are performed using CMG over a 21*21 grid system (see **Figure 5.1**) with a single well for a 2 phase (water and gas) production. The model represents an 80 acres drainage area of equally spaced grids. The coal-seam was considered to be sealed, homogeneous and isotropic in order to focus more on the parameters under investigation. The Langmuir sorption isotherm equation was used to model the pure component isotherms.

All sensitivity runs use some characteristic reservoir properties some of which are varied because they were found to be important in determining the outcome variables of interest. The initial set of sensitivity runs examined the effects of the coal seam properties such as matrix and fracture permabilities, fracture and matrix porosity, reservoir type (saturated and undersaturated), sorption time and adsorbed gas volume we have approximated different types of coals. And a base case data is also used as a basis for comparison for the sensitivity. The base case data is shown in Table 5.1.

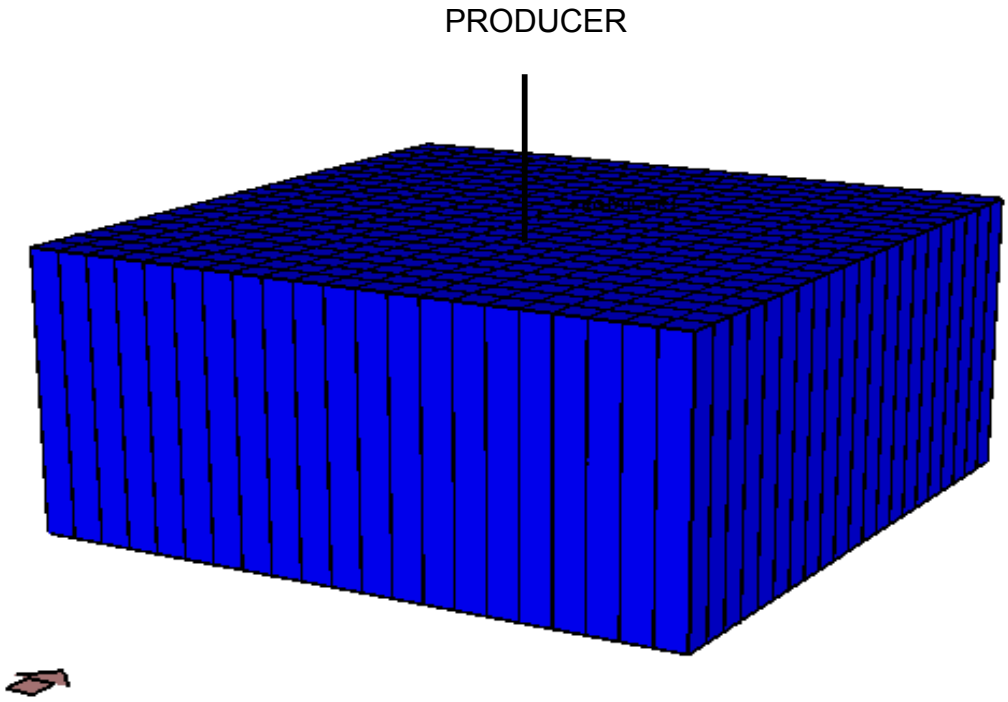

Figure 5.1- 21*21 Simulation model grid model.

Table 5.1- Base case coal reservoir properties		
Coal Properties		**UNITS**
Coal Seam Thickness	30	*ft*
Pay Depth	3280	*ft*
Fracture/Cleat Spacing	0.042	*ft (0.5 inches)*
Fracture Porosity	0.001	
Fracture Absolute Permeability	2	*md*
Fracture Compressibility	100E-06	$psia^{-1}$
Matrix Porosity	0.005	
Matrix Absolute Permeability	0.0001	*md*
Matrix Compressibility	100E-06	$psia^{-1}$
Water Density	62.4	lb/ft^3
Water Viscosity	0.607	*cp*
Water Compressibility	4E-06	$psia^{-1}$
Coal Density	89.5841	lb/ft^3
V_i, Langmuir Volume	0.23	*gmole/lb of rock*
p_L, Langmuir Pressure	725.189	*psia*
Disorption Time	10	*days*
Initial Reservoir Pressure *(Matrix)*	725.189	*psia*
Initial Reservoir Pressure *(Fracture)*	1109.54	*psia*
Initial Water Saturation *(Matrix)*	0.592	*fraction*
Initial Water Saturation *(Fracture)*	0.999	*fraction*
Initial Coal Gas Content	100%	
Diffusion Constant	0.000385806	cm^2/sec

During modeling of coalbeds using CMG, two relative permeability tables are specified for the matrix and fractures. The matrix relative permeability table is not used since the simulator disables all matrix-to-fracture Darcy flow when coalbed modeling is used, since the assumption is that the flow is a diffusive process; based on Fick's law.

Figure 5.2 shows the relative permeability curves used to model the matrix and the fracture flow.

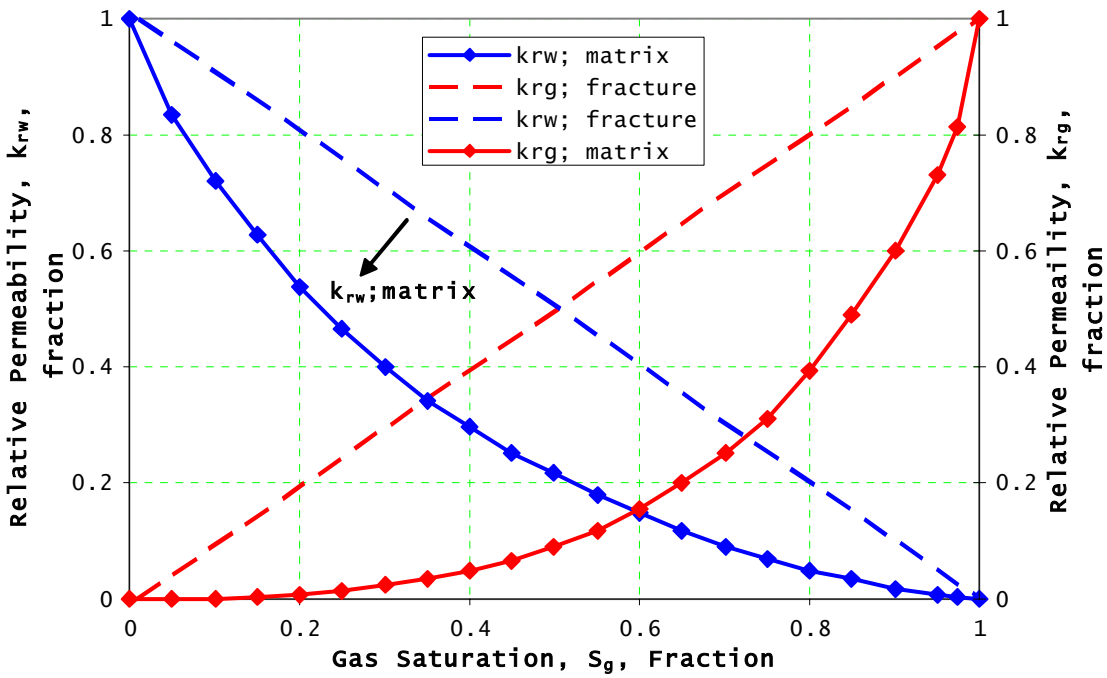

Figure 5.2- Gas and water relative permeability curve.

5.2 Sensitivity Analysis

In a sensitivity study, one parameter is varied while all other parameters are kept constant at some base values. The sensitivity analysis is conducted by varying the pertinent modeling parameters that affect coalbed methane gas production, using the base case 2

dimensional single well CMG model. The results of the simulation were analyzed to determine the primary performance of the coal-seam under these varying conditions for which varying these parameters would be similar to modeling different types of coal seams.

These initial set of runs examined the effects of the coal seam properties such as matrix and fracture permabilities, fracture and matrix porosity, reservoir type (saturated and undersaturated), sorption time and adsorbed gas volume. A total of 12 desorption times, 14 initially adsorbed gas volumes, 5 matrix porosities and 5 fracture porosities were investigated for this study. The coal-seam was considered to be sealed, homogeneous and isotropic in order to focus more on the parameters under investigation. The Langmuir sorption isotherm equation was used to model the pure component isotherms.

The sensitivity study provides a discussion of the physical production responses observed for each parameter sensitivity. Results from the simulation were obtained and analyzed, while focusing on indicators such as; peak gas rate and time to peak.

5.3 Effects of Coal Seam Modeling Parameters on Gas Rates.

Based on results from the sensitivity analysis, the direct effect of varying these coalbed methane parameters is studied. These results are also used to determine the independent and group relationship between some of these parameters and some key indicators such as the time to peak and peak gas rate using single and multiple regressional analysis.

The coal seam modeling parameters investigated in this work are desorption time, initially adsorbed gas, matrix and fracture permeability and the matrix and fracture porosity.

These simulation runs were undertaken for a certain range of varying values for coal-seam properties with respect to their base case values. Table 5.2 shows the data range for the different parameters under consideration.

Table 5.2 – Data range for input modeling parameter for sensitivity analysis

		DATA RANGE		
	INPUT PARAMETER	BASE	LOW	HIGH
1.	Desorption time (τ), *days*	10	0.5	100
2.	Initially adsorbed gas (V_i), *scf/rcf*	8.5	8.5	3735
3.	Fracture system permeability, *md*	2	0.01	100
4.	Fracture porosity ϕ_f, *fraction*	0.001	0.001	0.1
5.	Matrix porosity ϕ_m, *fraction*	0.005	0.001	0.1

5.3.1 Desorption Time

Sensitivity that confirms results from previous work by authors like Zuber [19] was conducted by varying the desorption time which in essence means modeling various types of coal. Desorption times in the range of 2 to 200 days was simulated. Fast desorption rates represented by low disorption time values are seen to show high gas rates

and peak gas production, **Figure 5.3**. Water rates are not as sensitive as the gas rates are to changes in desorption times but **Figure 5.4** shows that for the first 100 days the dewatering stage (process of producing water from the cleats), the small desorption times have low water production rates as compared to higher desorption values.

A very interesting effect of importance was observed in the sensitivity runs and this is the double peaks that existed for cases of low desorption times (fast diffusion) of 2. The cause of this effect is still under investigation.

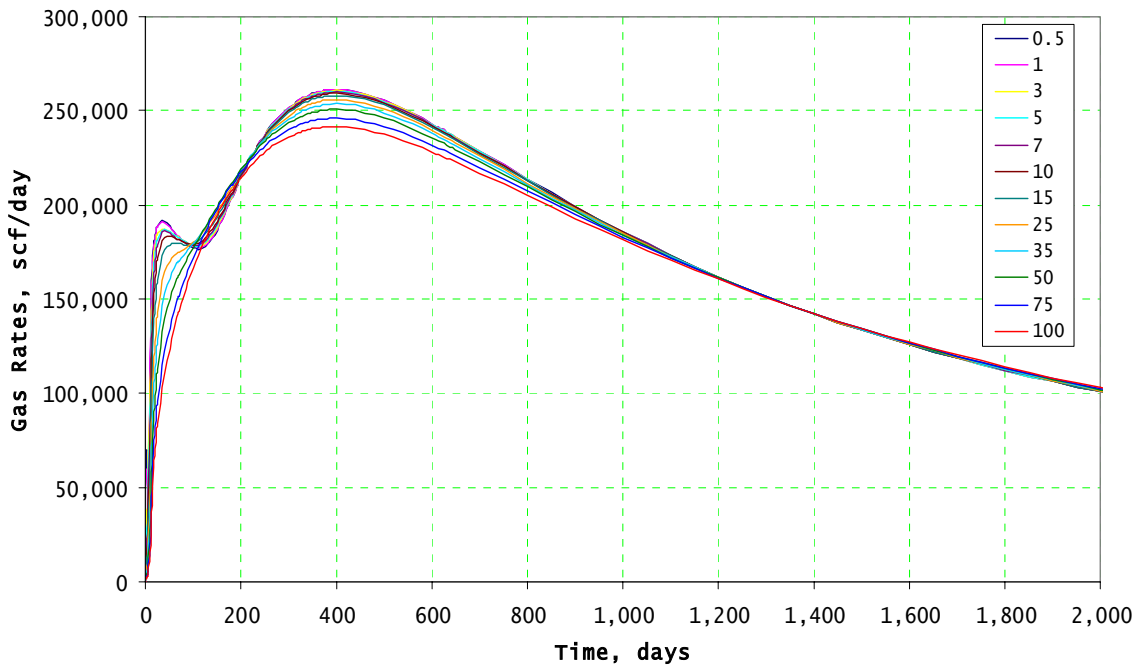

Figure 5.3- Effect of desorption time on gas for varying only the desorption time τ.

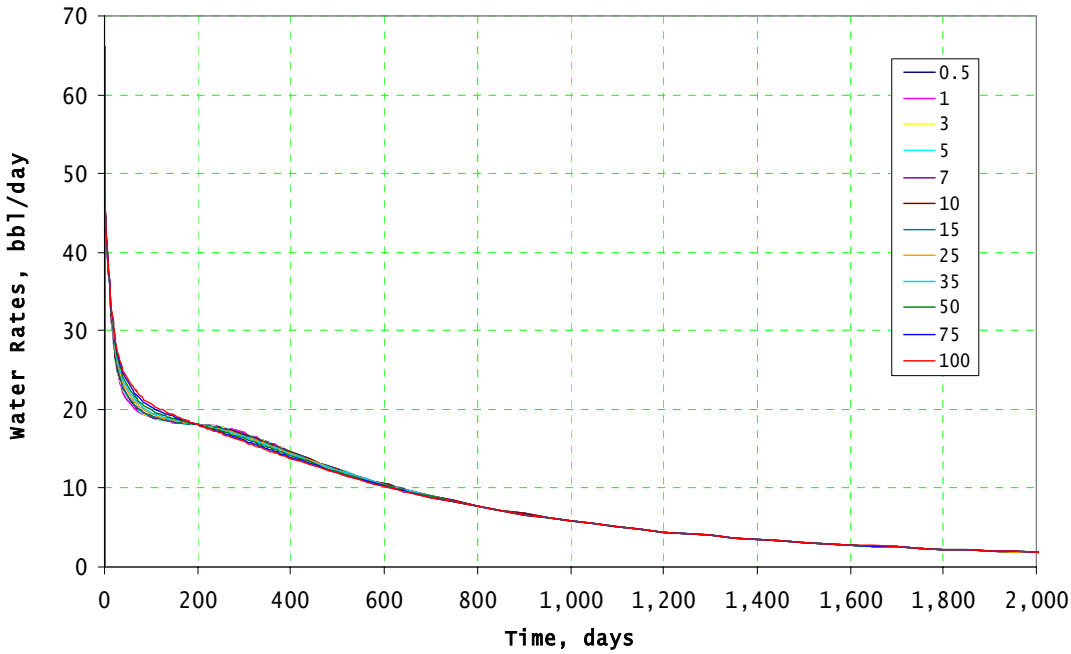

Figure 5.4- Effect of desorption time water rate for varying only the desorption time, τ.

5.3.2 Matrix Permeability

Permeability is a very important parameter and has probably one of the largest effect on flow rate and recovery. In the modeling of coalbed methane reservoirs using CMG, two separate permeability values are defined for the matrix and the fracture. The matrix permeability in CMG is not actually used in computations, "since the simulator disables all matrix to fracture Darcy flow when coalbed modeling is being used, a positive values is only used to indicate that there is a pathway for diffusion to occur between matrix (coal) and fracture (cleats)" [18]. To confirm this modeling concept, simulation results in **Figure 5.5** show that varying the matrix permeability does not show any changes in the gas rates.

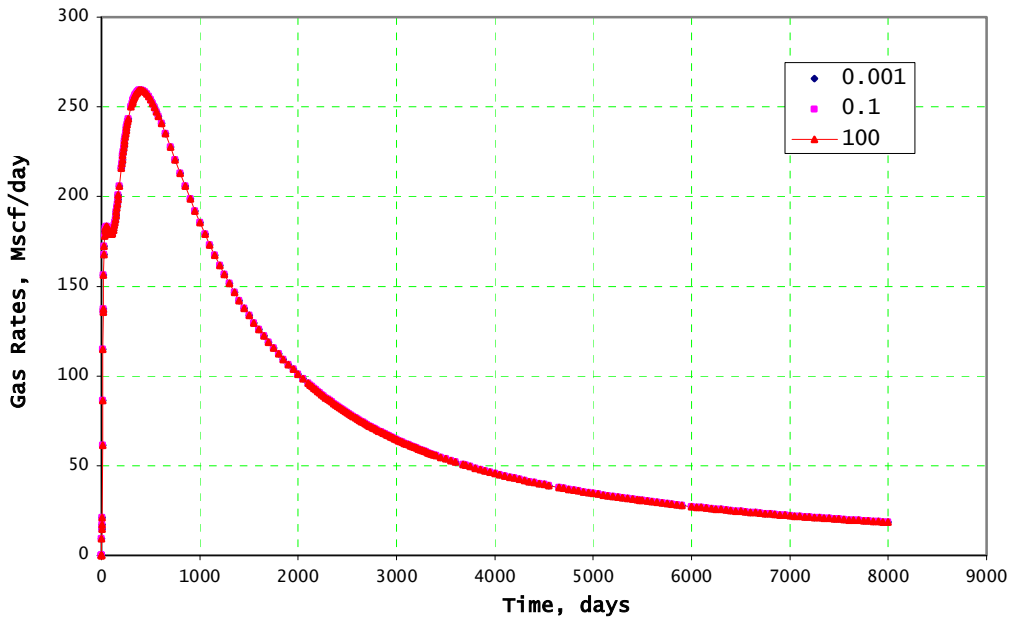

Figure 5.5- Simulation results showing that varying the matrix permeability does not affect the gas rate.

5.3.3 Fracture System Permeability

The fractures are the main conduit for flow in coalbeds, this makes the fracture system permeability a very important parameter for simulating the darcy flow in the fractures. **Figures 5.6 & 5.7** shows that gas and water production rates increases with increasing fracture permeability with all other reservoir parameters being kept constant. As the permeability increases with the gas peak rate, the time to peak is also seen to be decreasing. This is probably because the pressure is being lowered more effectively.

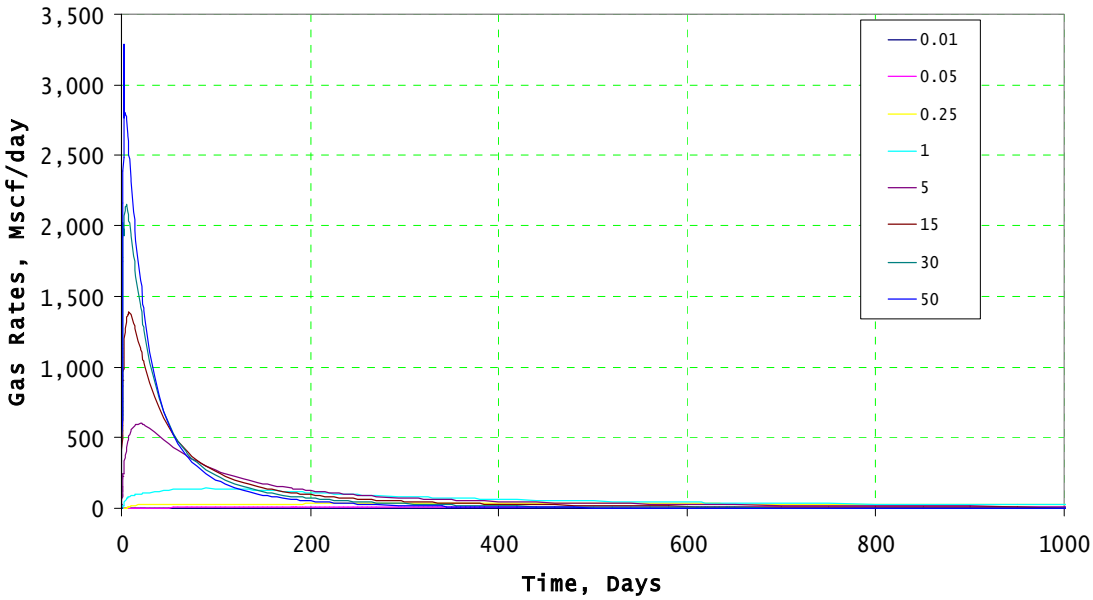

Figure 5.6- Simulation results show that gas production rate increases with increase in the permeability.

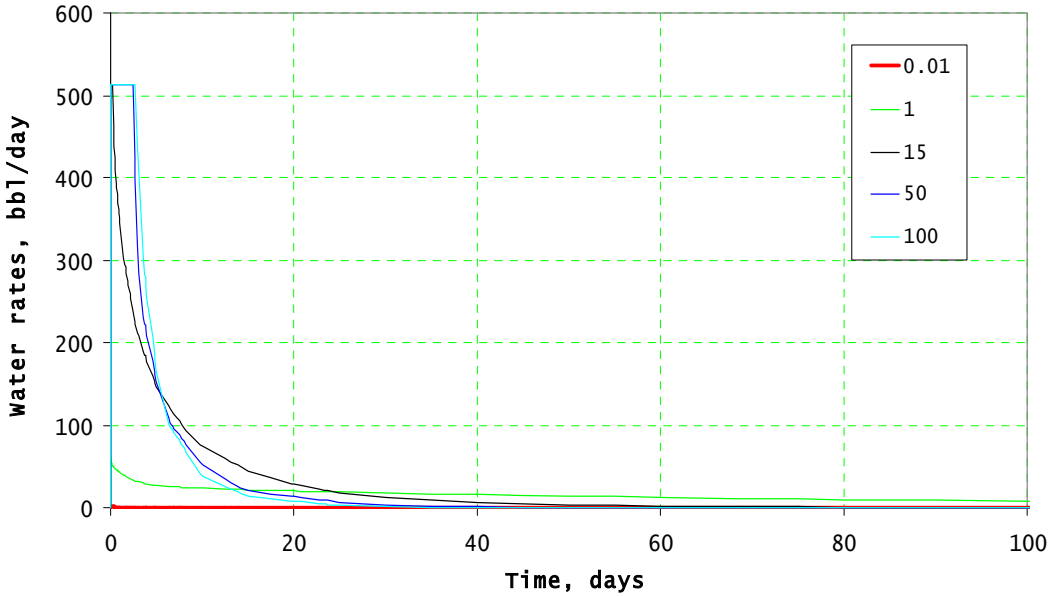

Figure 5.7- Simulation results show that water production rate increases with increase in the permeability.

5.3.4 Coal Matrix Porosity, ϕ_m

Increasing the value for coal porosity increases the pore volume and the surface gas (which is the adsorbed volume plus the free gas in the matrix pores) and decreases the bulk volume where the gas is sorbed.

As the porosity is increased, the adsorbed gas volume is decreased. Table 5.3 which we would expect to give decreased rates, since it's assumed in this type of coal models that 99% of the gas is adsorbed and only the adsorbed gas is desorbed and produced, but simulation results show the contrary in **Figure. 5.8**. The gas rates are actually increasing with increase in the porosity from 0.001 to 0.1 even though the adsorbed volume of gas is decreasing. The reason for this increase in gas rates could be as a result of the increase in the surface gas, which means that the simulator actually flows the gas which exists in the pores of the matrix. This is contrary to the manual which states that "when coalbed methane modeling is being used, since coalbed modeling inhibits matrix-to-fracture Darcy flow for both gas and water, there seems little point in modeling water saturations within the matrix (coal) as such water will not be produced"[18]. So the assumption is that whatever fluid; water or gas initialized in the matrix pores will not flow, but we find that this is not entirely correct, see **Figure 5.8.** Increasing the porosity, consequently increasing free gas in the matrix actually increases gas rates. This means that CMG actually flows the free gas in the matrix, but mostly likely using the diffusion flow equations that it utilizes for the adsorbed gas. **Figure 5.9** shows that the water production rate is insensitive to the changes in matrix porosity, most likely because there is no water stored or being flowed from the matrix pores.

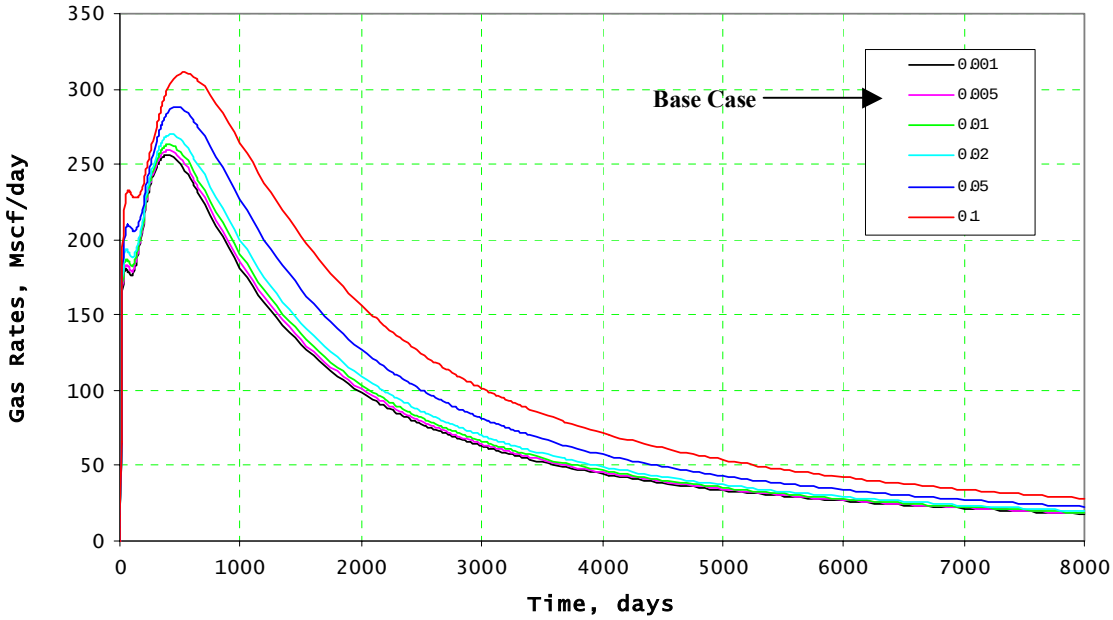

Figure 5.8- Simulation results show that gas production rate increases with the matrix porosity.

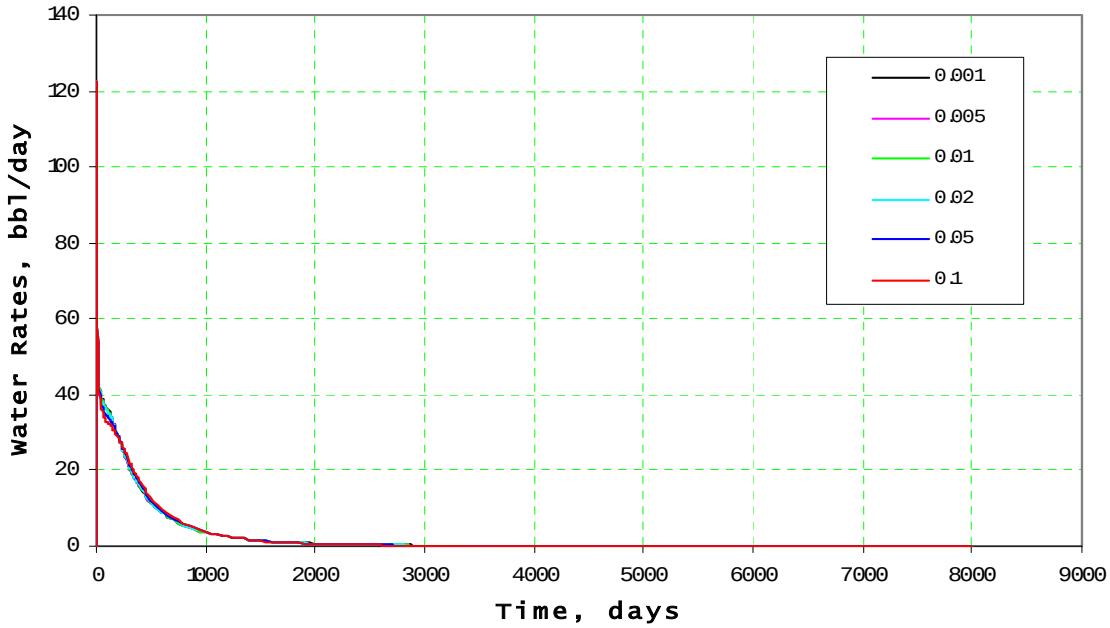

Figure 5.9- Simulation results show that water production rate is not sensitive to change in the matrix porosity, since there is no water stored in matrix pores.

Table 5.3- Effect of variation in coal matrix porosity on the adsorbed gas and surface gas volumes						
	COAL MATRIX POROSITY					
	0.001		0.005		0.1	
	MATRIX	FRACTURE	MATRIX	FRACTURE	MATRIX	FRACTURE
Pore Volumes						
Total Pore Volume, rft^3	100	104.54	502.13	104.54	10043	104.54
Originally in Place						
Adsorbed Gas. MMscf	884.6	0	881.2	0	800.31	0
Surface Gas. MMscf	889.47	8.042E-04	905.56	8.042E-04	1287.60	8.042E-04
Surface Water, MSTB	1.792E-04	18.68	8.96E-04	18.68	1.792E-04	18.68

5.3.5 Fracture System Porosity, ϕ_f

The porosity used in the simulator is the ratio of the volume of the fractures, or macro porosity to the bulk volume. The fractures are not used as storage for free gas in these model, but instead they are important as a storage site for water. Seidle and Arri[8] showed that for most coal basins throughout the world, coal release their adsorbed gas rapidly and coal degasification is rate limited by gas flow in the cleats. So the fracture system porosity has a significant effect on the flow capacity of a coal reservoir. Variations in fracture porosity within a range of 0.001 to 0.1 were simulated for the base case, which is assumed to be fully saturated with water. For a lower coal porosity of 0.001 the peak gas rate were higher while the higher coal porosity of 0.1 is seen to constrain the gas rate due

to the large pore volume (**Figure 5.10**). Lower coal porosities also give lower water rates when compared to higher values **(Figure 5.11)**. This also means that they dewatering process is faster in these low porosity coals.

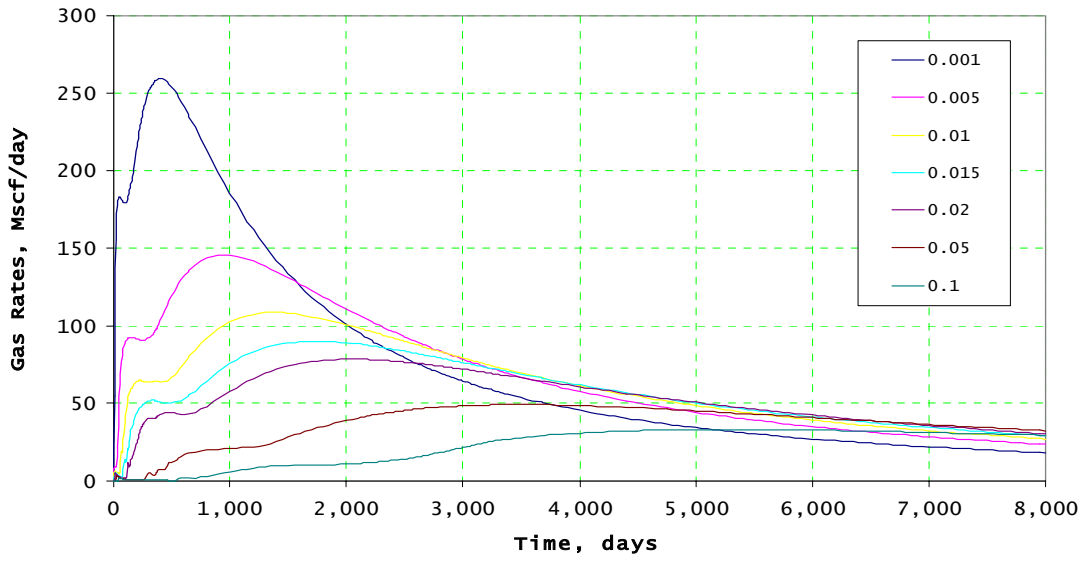

Figure 5.10- Simulated gas production for variation in the fracture porosity shows increase in the production rate with decrease in porosity.

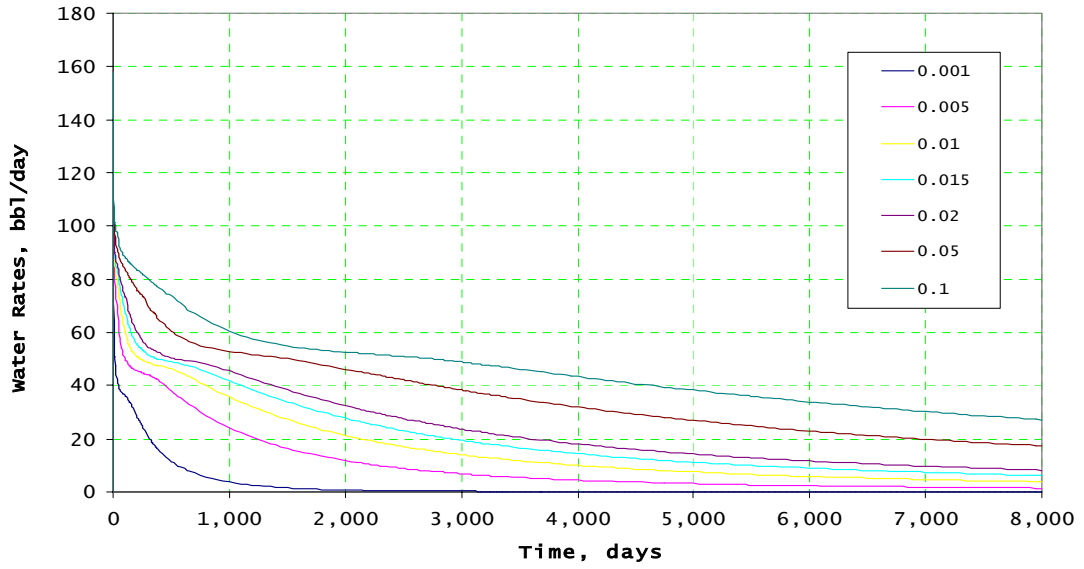

Figure 5.11- Simulated water production rates, shows significant effect of variations in the fracture porosity. The increase in the fracture porosity increases the water rates.

5.3.6 Initially Adsorbed Gas

The coal matrix gas content refers to the amount of gas that exists in coal as adsorbed gas. When using the black oil formulation for coalbed reservoir simulation, the amount of gas adsorbed in a unit volume of coal is equated with the amount of gas dissolved in a black oil at a given pressure[21].

The flow capacity of the coal is also found to be greatly influenced by this parameter. A wide range of values from 8.5 to 3735 scf/cu.ft was investigated to model a wide range of coal ranks **Figure 5.12**. As expected, the increase in the matrix gas content increases the gas production rate, since more gas is in storage in adsorbed form.

An obvious occurrence of double peaks is seen in the simulation results shown in **Figure 5.12,** for cases of gas content within the range of 8.5 scf/cu.ft to 2241 scf/cu.ft.

Analyzing the trend of the double peaking, we see that as the gas content increases, the first peak becomes more evident and the second peak actually disappears at a gas content of 2988 scf/cu.ft. This is probably because there is more gas adsorbed and when the well is put on production, a lot of gas is desorbed initially and the gas production peaks out much earlier. These results show that the double peaking feature is actually affected by the initial matrix gas content. The water rate in **Figure 5.13** is seen to be decreasing with increase in the gas content.

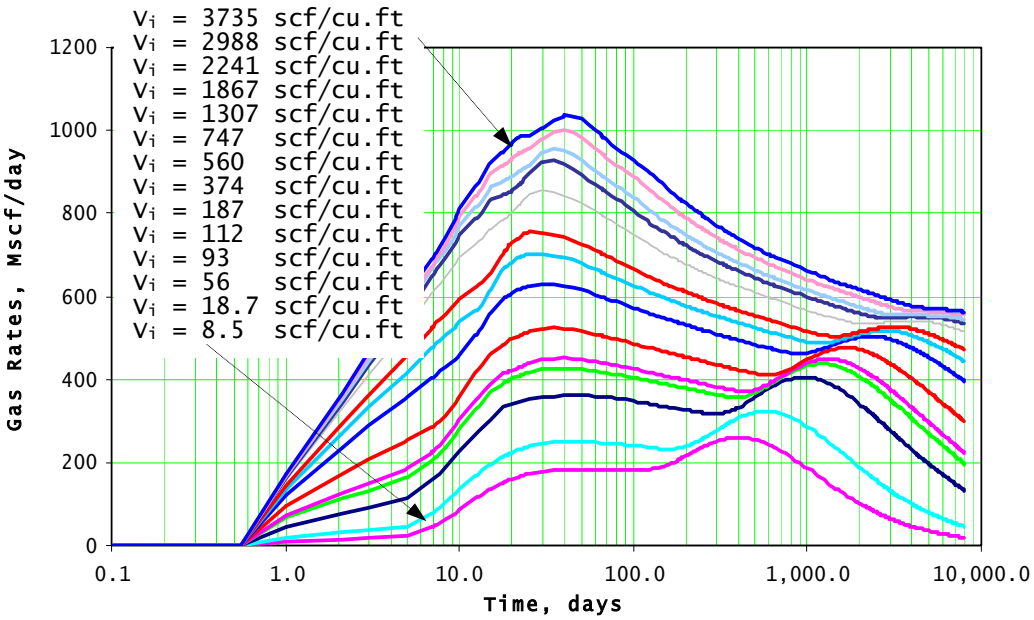

Figure 5.12- Simulation results show the first peak becoming more evident as the matrix gas content increases and the second peak diminishes.

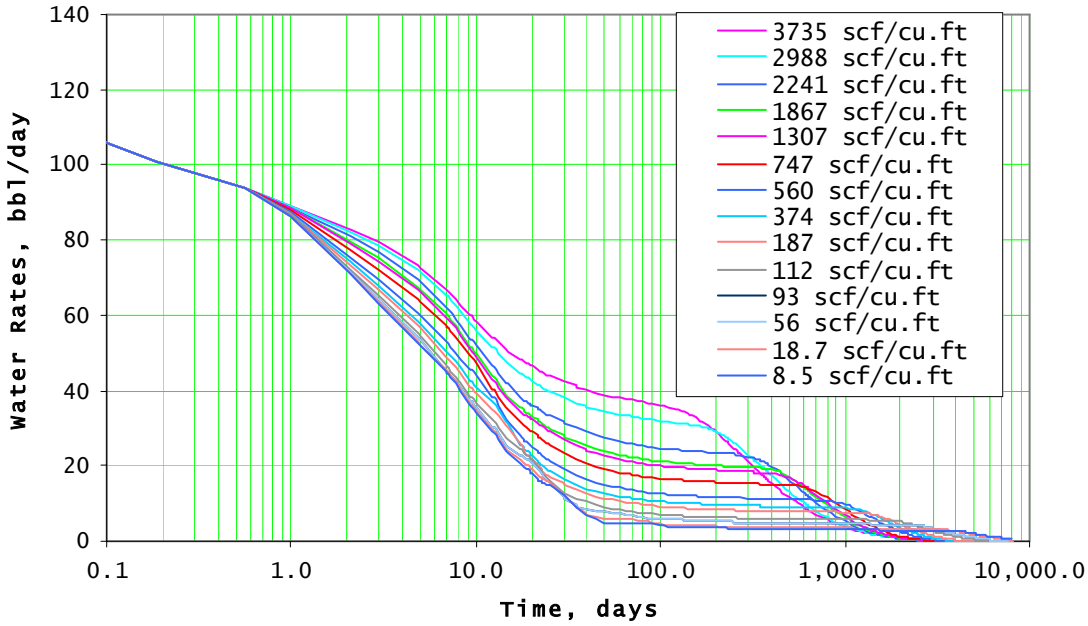

Figure 5.13- Simulation results show the low gas content coals with higher water rates as expected.

5.3.7 Saturated and Undersaturated Coalbed Methane Reservoirs

To determine whether a coal seam is saturated or undersaturated would depend on the desorption pressure relative to the initial reservoir pressure.

A saturated coal is seam is a coal seam that is holding as much adsorbed gas as it can possibly hold under the given reservoir pressure and temperature. This is analogous to an oil reservoir with its initial reservoir pressure at the bubble point pressure. This saturated state is obtained in the model by initializing the matrix pressure to be equal to the fracture pressure.

For an undersaturated coal seam, the pressure at which the gas starts to desorb which is the same as the matrix pressure, is less than the reservoir pressure which is rpresented by the fracture pressure.

Simulation results show that the initial state of the reservoir on production only has a short term effect on the gas production rates. From the results, it can be observed that for all cases of varying initial adsorbed gas, V_i **(Figure 5.14)** and desorption time, τ **(Figure 5.16)** saturated reservoirs give higher gas rates as compared to undersaturated cases for the first couple of days (<100 days). This is most likely because the gas starts to desorb instantaneously, as soon as the well is put on production unlike the undersaturated case where the fracture pressure has to be depressurized to the matrix pressure for the gas to desorb. The water production rates in **Figures 5.15 & 5.17** show higher rates for the undersaturated cases and lower rates for the saturated cases. This is because of the

instantaneous gas production in the saturated cases as compared to the undersaturated cases.

In summary, we can infer based on the analysis that the effect of the initial state of the reservoir; saturated or undersaturated is only felt within the first few days of production, and therefore, is not as important as we had earlier anticipated. So for the generalized correlations described in Chapter VI it was assumed that the reservoir is initially undersaturated.

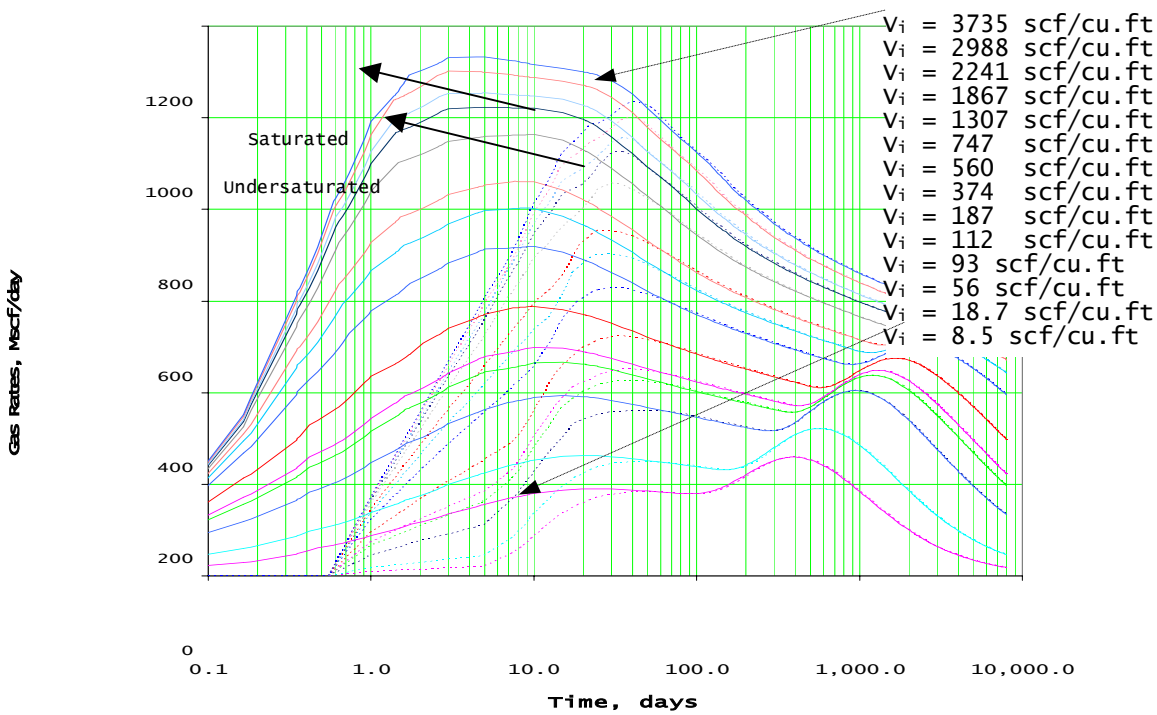

Figure 5.14- Simulation results show the gas rates and the effect of reservoir type; saturated or undersaturated of various V_i (initial gas adsorbed volume) values.

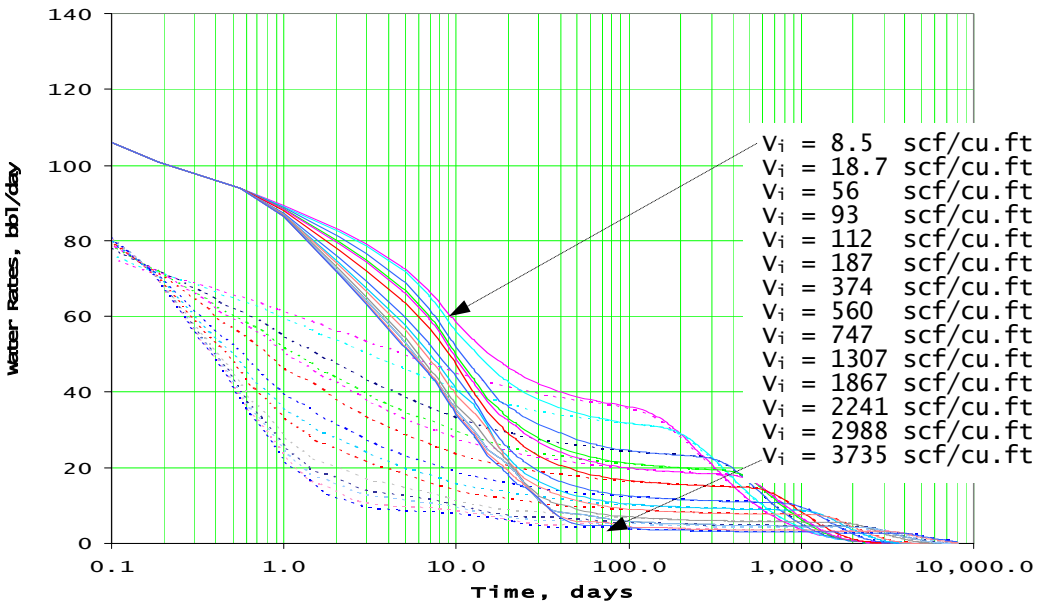

Figure 5.15- Simulation results show corresponding higher water rates for undersaturated cases when compared to the saturated cases for various V_i (initial gas adsorbed volume) values.

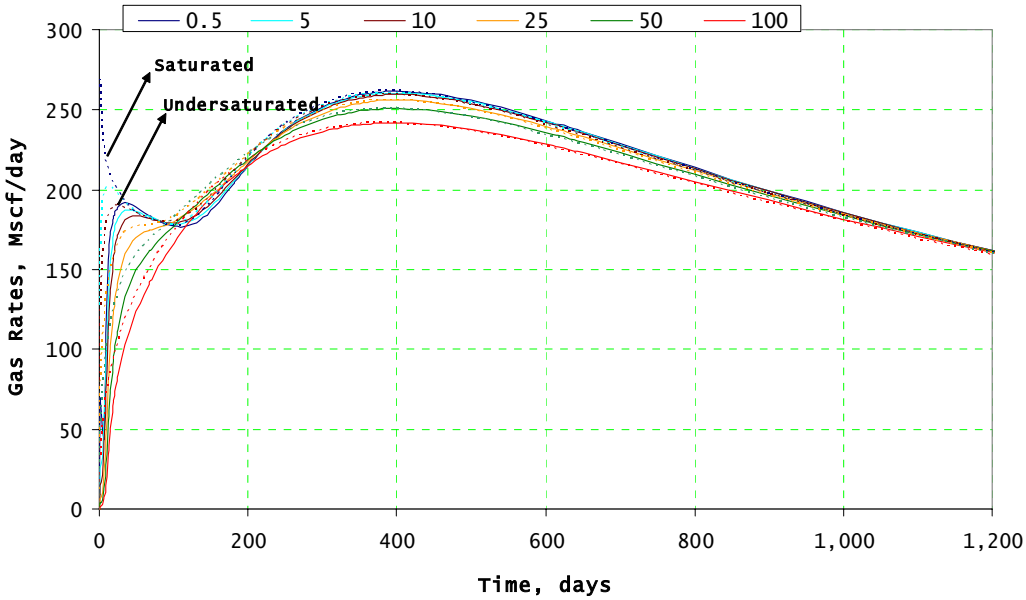

Figure 5.16- Simulation results show the effect of reservoir type; saturated or undersaturated on the desorption time.

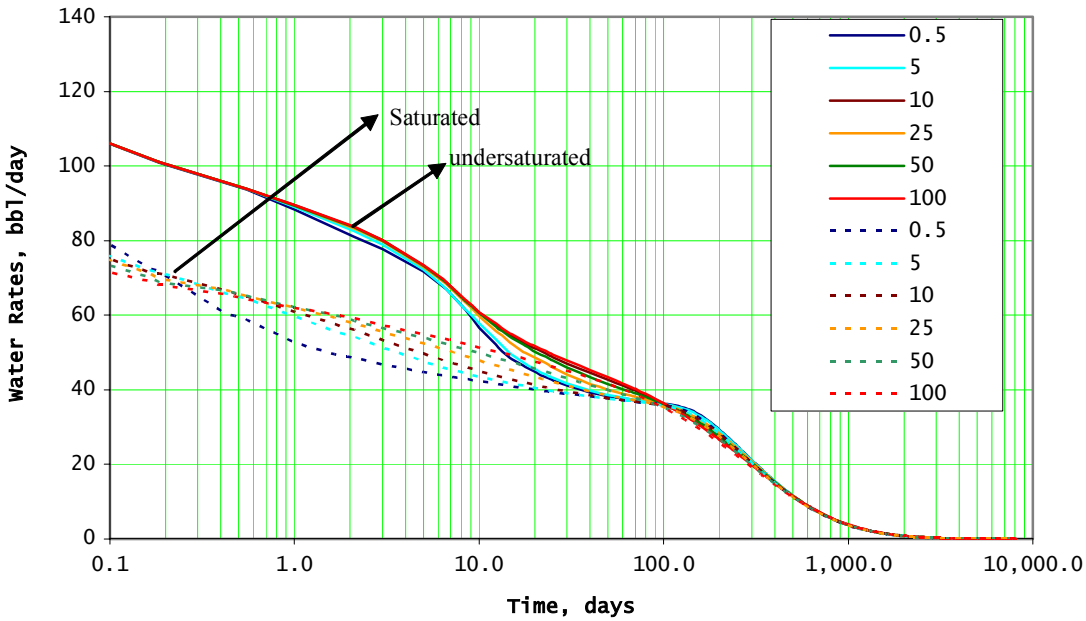

Figure 5.17- Simulation results show corresponding higher water rates for undersaturated cases when compared to the saturated cases for various desorption time, τ values.

5.4 Investigating the Dual Peaking Behavior

To understand the dual peaking behavior and reason for its occurrence, the gas saturation profile for a typical dual peaking case; V_i = 2.5 scf/day was investigated. We see that the 1st peak at 40 days (**Figure 5.18**) and also as can be seen from the gas saturation profile in **Figure 5.19** occurs before the fracture pressure in the boundary (grid block 21 11 1) is depressurized to the matrix pressure and gas starts to desorb and flow into the fractures. Also the 2nd peak at 1200 days occurs after the boundary effect has been felt i.e. that is, fracture pressure in the boundary grid blocks have been depressurized to the matrix pressure by producing the water in the fractures.

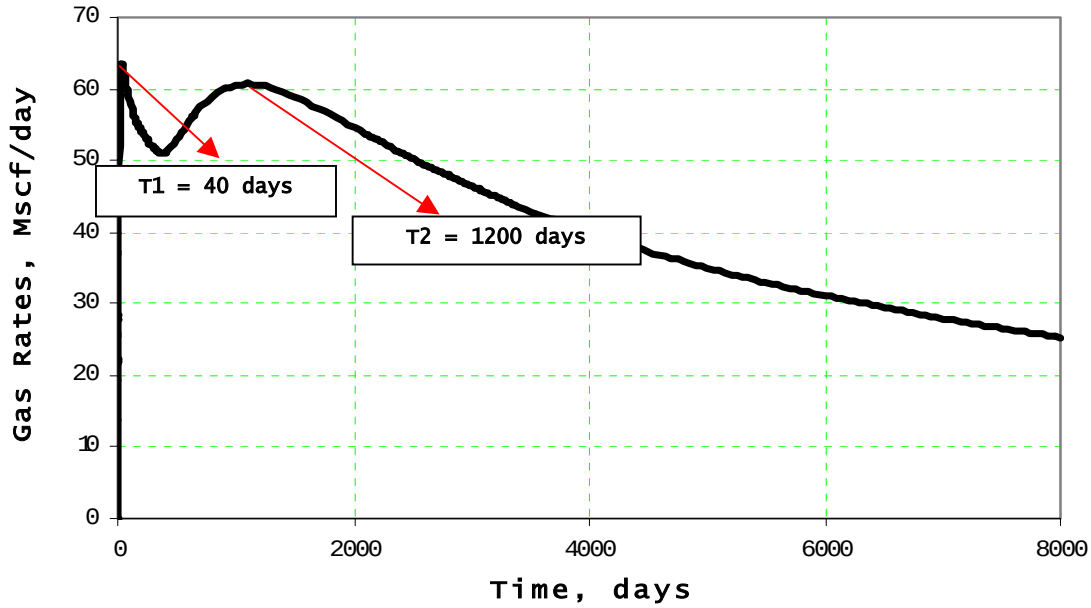

Figure 5.18- Simulation results for gas production from a typical dual peaking case of V_i =2.5 scf/day and τ = 10 days.

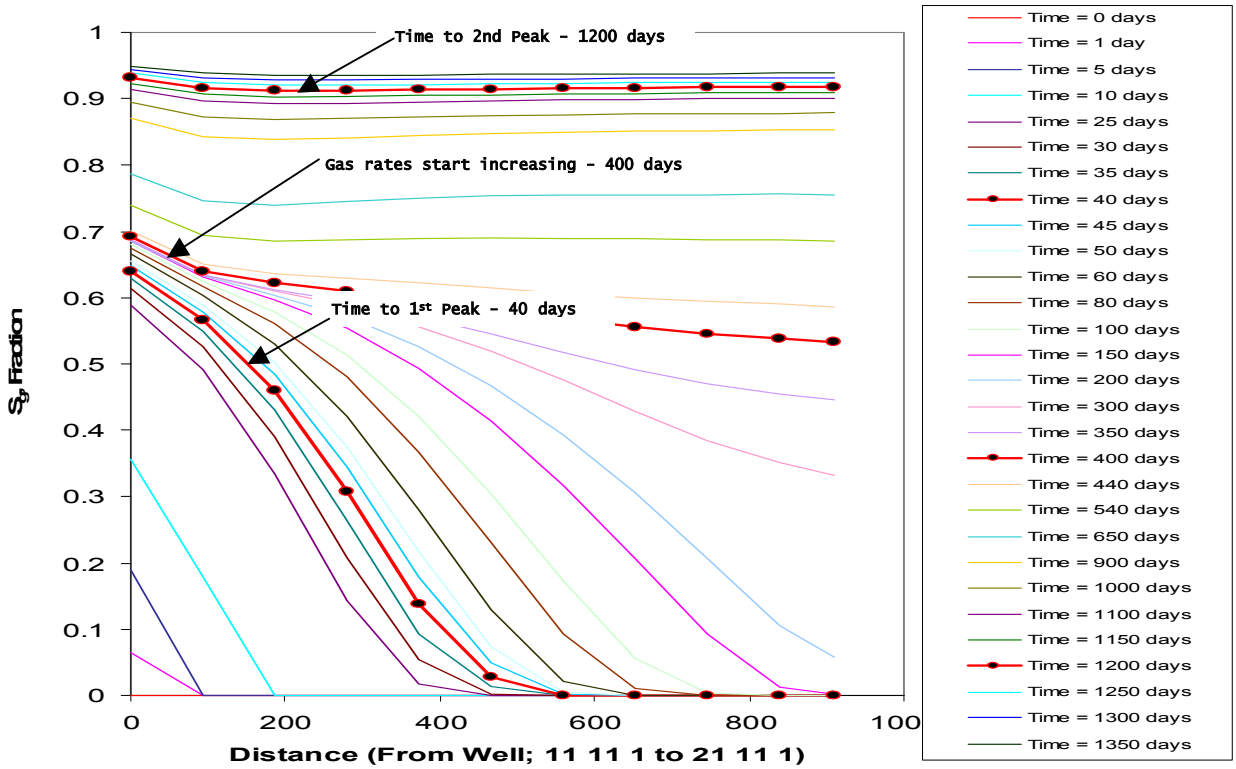

Figure 5.19- Gas saturation profile, showing that the 1st peak occurs before fracture pressure in the boundary grid blocks are depressurized to the matrix pressure. And the 2nd peak occurs after the boundary effect.

CHAPTER VI

GENERALIZED CORRELATIONS

6.1 Dual Peaking

Simulation results indicated a unique feature referred to as "dual peaking" in the gas rate curves. This unique behavior has also been seen in real field production data. **Figure 6.1** shows a typical dual peaking case from reservoir simulation results of the base case 21*21*1 single well model and **Figure 6.2** shows the corresponding water rates

Chaianansutcharit[4] reported that the dual peaking behavior arises if the drainage boundaries are not influenced at the same time. They also showed that the dual peak behavior is not seen if the drainage area is scaled according to the permeability anisotropy. For a square drainage area, they showed that if the permeability is anisotropic, the gas rates will exhibit a dual-peak behavior and a single peak for isotropic cases, see **Figure 6.3.** Simulations results from this work show that for an isotropic, square drainage area a dual peak can still exist. And this is in contrast with results shown in **Figure 6.3** which show that an isotropic, square drainage area does not exhibit dual peaking but has only a single peak.

A sensitivity analysis was conducted to determine which modeling parameters had the most effect on the dual peaks and could be incorporated into the generalized correlations. Details of results from the sensitivity analysis are discussed in Chapter V.

The major modeling parameters that were considered to be important for these correlations are the initial gas adsorbed (V_i), the desorption time (τ), fracture porosity

(ϕ_f) and matrix porosity (ϕ_m). To generate data needed to perform the simple and multiple regression analysis, a total of 39 simulation cases for various values of the modeling parameters were run, to determine the time to 1st peak (t_1), magnitude of the 1st peak (q_1), time to 2nd peak (t_2) and magnitude of the 2nd peak (q_2). Data generated from simulation runs can be seen in Appendix C; Table C-1.

This work shows the effect of other factors such as the modeling parameters on the dual peaks and how these modeling parameters could be used to determine the time and magnitude of the peaks.

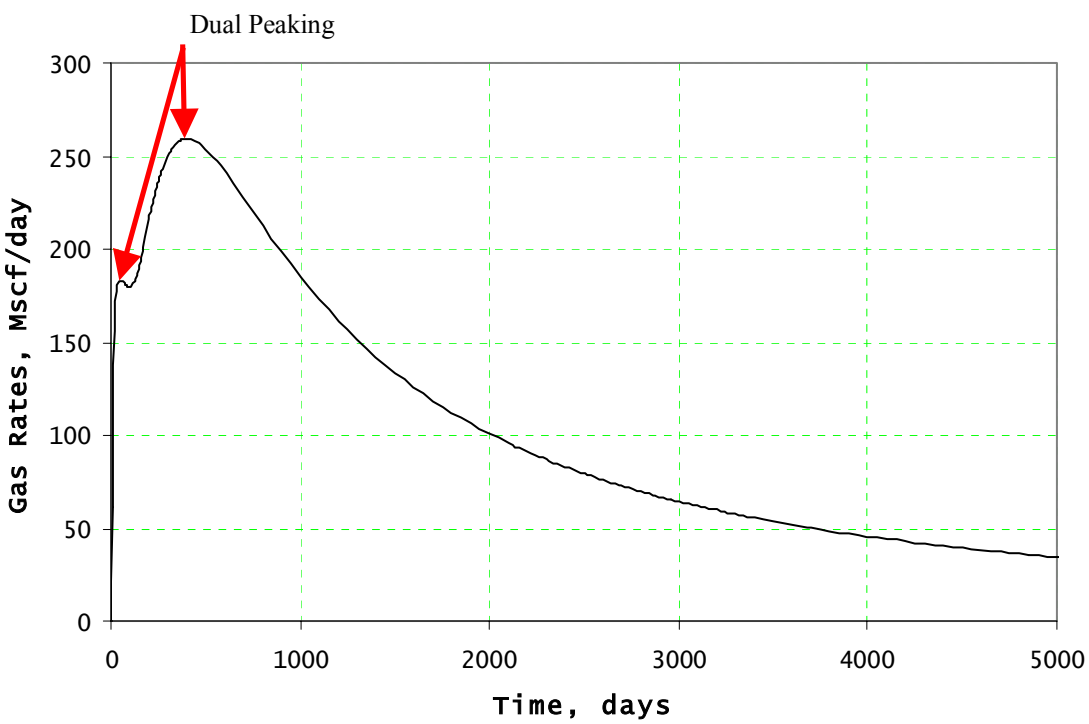

Figure 6.1- Simulated CBM gas production showing the double peaks of gas rates.

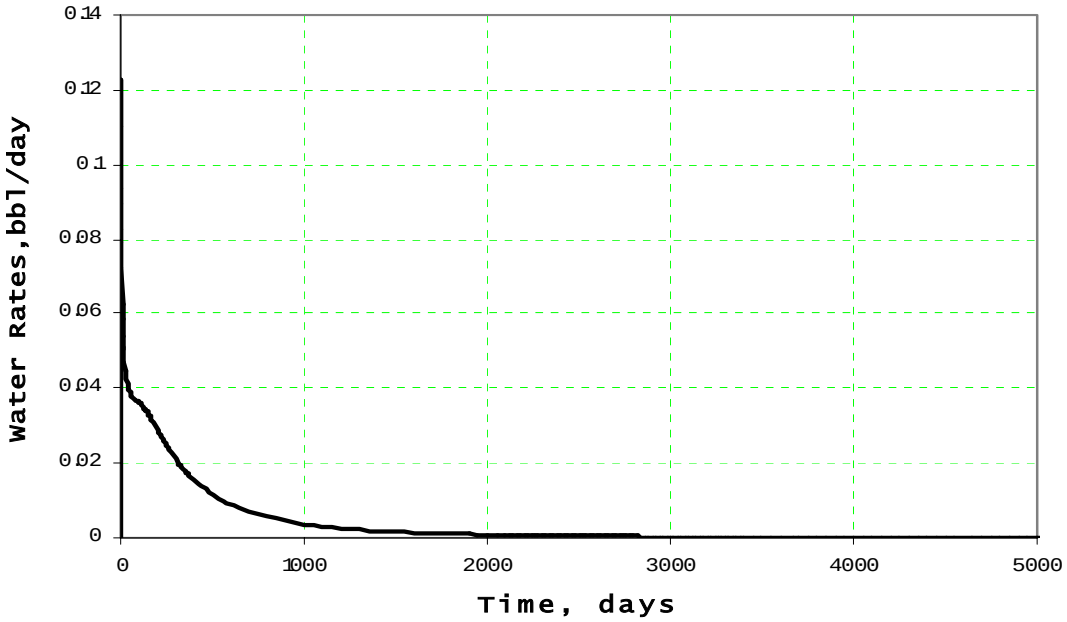

Figure 6.2- Simulated CBM water production rates showing a continuous decline in the water rates after the 1st peak.

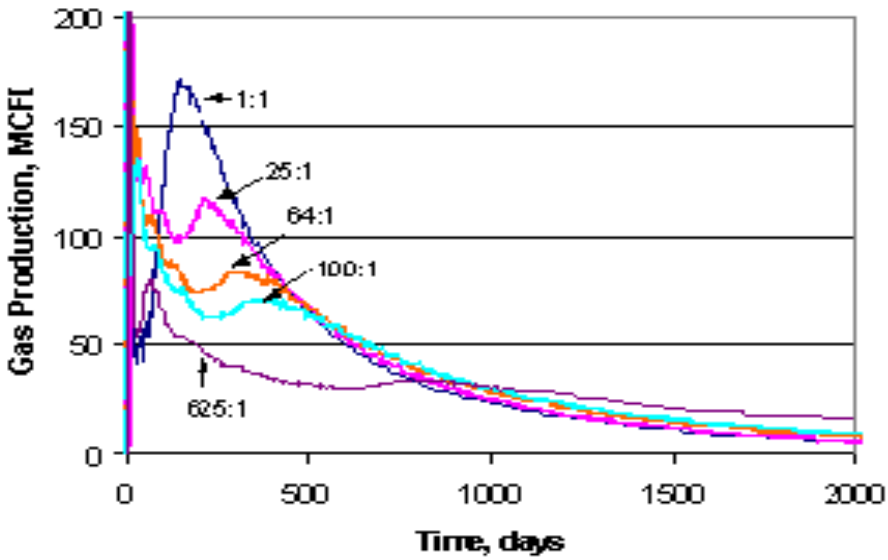

Figure 6.3- Impact of permeability anisotropy on gas flow rate, shows that for an isotropic square drainage area there is no dual peaking[4].

6.2 Simulation Base Case

Figure 6.1 presents the base case simulation results for the gas production for which the input data is given in Table 5.1. The trend of the gas production shown in **Figure 6.1** is typical of a CBM reservoir. Once the well is put on production an instantaneous increase is seen in the water and gas production as a result of the change in the bottom hole pressure. After a couple of days, we see a decline after the surge and another increase to a maximum gas rate and a decline. The water rates also decline continuously after the first peaking.

6.3 Generalized Correlations

The generalized correlations are developed based on data from simulation results using simple and multiple regressional analyses. Four parameters variables (or dependent variable); time to 1st peak (t_1), peak gas rate at first peak (q_1), time to second peak (t_2) and the peak gas rate at second peak (q_2) were determined to be most important in determining when a well will peak and its corresponding peak gas rate. In this work, 4 correlations were developed to compute the 4 parameters variables as functions of a combination of the desorption time, initially adsorbed gas volume, matrix porosity and the fracture porosity. And these are referred to as the modeling parameters (independent variables).

The generalized correlations were developed on the basis of the relationship of the modeling parameter as independent variables with the 4 parameter variables; t_1, q_1, t_2 and q_1.

6.3.1 Simple Linear Regression

Using simple linear regressional analysis this work investigated how each of the modeling variables in the parameter group varied independently with the four different parameters variables. Linear regression is used to examine the relationship between a dependent variable and an independent or predictor variable. Linear regression enables you to find the equation by which you can best predict scores on the dependent variable from scores on the predictor variable. Plots in Appendix C; **Figures C-1 through C-16,** shows the results from the simple regressional analysis of the modeling variables and each of the parameters variables. Table 6.1. shows the different equation forms from the simple linear regression that represent the relationship between the parameter variables, t_1, $q1$, t_2 and q_2 and each of the modeling parameters, V_i, τ, ϕ_f and ϕ_m.

Table 6.1- Simple linear regression equations				
Parameter Variable	Modeling Parameters			
	V_i	τ	$\varnothing_f$	$\varnothing_m$
t_1	$20.4+29.8*EXP(-0.0051*V_i)+0.08*V_i^{0.68}$	$0.35*\tau^{1.59}+34$	$21156.8*\varnothing_f+26.2$	$216.25*\varnothing_m+48.3$
q_1	$197852*V_i^{0.20}$	$-792.32*\tau+191269.8$	$6926.26*\varnothing_f^{-0.45}$	$393.5*EXP(\varnothing_m*3.15)$
t_2	$310*V_i^{0.34}$	Constant=400 days	$19073.7*\varnothing_f^{0.56}$	$508916*\varnothing_m+182260.1$
q_2	$38502*LN(V_i)+268861.5$	$-201.4*\tau+261362.3$	$15287.5*\varnothing_f^{-0.411}$	$258057.1*EXP(\varnothing_m*1.92)$

6.3.2 Multiple Regression

Multiple regression is used to understand a phenomena by examining how variables correlate on a group level by exploring the relationships between the multiple independent variables in a sample. And while theory is useful for identifying what variables should be in a prediction equation, the variables do not necessarily need to make conceptual sense.

In this work a sample data set (see Appendix C: Table C-1), that reflects the various independent variables is used to create a regressional equation that would optimally predict the parameter variables t_1, t_2, q_1 and q_2. The data in Appendix C: Table C-1 represents a variety of conditions. The desorption time ranges from 0.5 days to 100 days, initially adsorbed gas volume (V_i) ranges from 8.5scf/rcf to 3735scf/rcf, matrix porosity (ϕ_m) ranges from 0.001 to 0.1 and the fracture porosity (ϕ_f) ranges from 0.001 to 0.1.

The modeling parameters are incorporated into four different parameter groups (that are representative of the parameter variables) on the basis of their relationship as independent variables.

To determine the best forms in which each of the modeling parameters can exist in the predictive equation a multiple regressional software called SAS, is used to guess the best forms of equation that would give the highest *r squared* value and the *C(p)* value (which is a measure of goodness of an equation).

The SAS software is initialized with equation forms realized from the simple linear regression analysis (see Table 6.1). After determining the best equation forms for which

the individual modeling parameters best fits in the predictive equation, Microsoft solver is used to compute the regressional coefficients that provides a minimization of deviations (residuals) between predicted and observed values for the data set. It also provides an optimization of the correlation between the predicted and observed simulation results. The final equation form would comprise of all the modeling parameters necessary to predict the parameter variable.

The *r-squared* value for each predictive equation is also calculated to measure the degree of linear relationship between dependent and the independent variables. The smaller the residual values around the regression line relative to the overall variability the better our prediction and the higher our r-squared value. It is a descriptive measure between 0 and 1 and the definitional formula for r-squared (r^2) is as follows for t_1;

$$r^2 = 1 - \frac{\sum (t_1 - t_{1\,EST})^2}{\sum (t_1 - \overline{t_1})^2} \qquad \text{.....} \quad 6.1$$

The predictive equations for computing t_1, t_2, q_1 and q_2 are as follows;

$$t_1 = \left[20.1 + 41.2(631e^{-1.15V_i} + 137V_i^{-0.43}) * \tau^{1.03*} * \phi_f^{0.98} * \phi_m^{0.202}\right]^{1.16} \qquad \text{.....} 6.2$$

$$t_2 = 0.029\left[2500\ E06 * V_i^{0.49} * \phi_f^{0.63} * e^{1.89*\phi_m}\right]^{0.84} \qquad \text{.....} 6.3$$

$$q_1 = \left[0.95 * (2408\ \tau + 1.037\ E05)V_i^{0.54} * \phi_f^{1.02} * (\phi_m + 789)\right]^{0.5} \qquad \text{..} 6.4$$

$$q_2 = \left[0.178*(-5046\tau + 1.629E06)*(5.426E07LN(V_i) - 4.917E07)*\phi_f^{1.036} * e^{2.94*\phi_m}\right]^{0.4}$$

$$\text{.....} \quad 6.5$$

The first correlation establishes the relationship between the t_1, time to 1st peak and a parameter group consisting of the modeling parameters V_i, τ, ϕ_f and ϕ_m. The generalized

correlation equation for t_1 in Equation 6.2 shows the degree to which each of the modeling parameters affect t_1. Fracture porosity and desorption time seems to have a greater effect on the time to 1st peak than the initial adsorbed gas and matrix porosity. This can also be seen by their powers in the predictive equation (Equation 6.2). The plots shown in **Figure 6.4a** & **Figure 6.4b** represents the same correlation, where **Figure 6.4b** is for increased gas rates.

The predicted values which are the values based on the correlation equation is plotted against the observed values from simulation results. **Figure 6.4b** shows that the predictive equation works the most for cases where only the fracture porosity is varied; represented by the legend 'Varying Fracture Porosity' in the plot .

For these set of correlations the sample data (Table C-1) was generated by varying one modeling parameter at a time while keeping the others constant. To test the predictive equation, simulation results for varying only one parameter and also more than one parameter at a time where compared with times calculated based on the predictive equation. This comparison is shown in **Figure 6.5**. The simulation data cases for the test are tabulated in Table C-2.

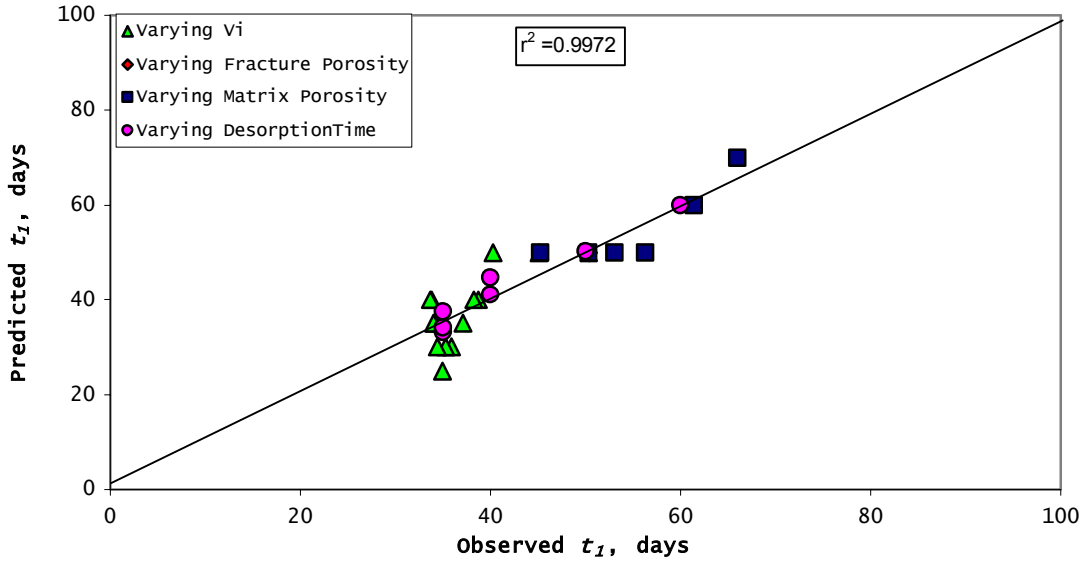

Figure 6.4a- Generalized correlation for t_1.

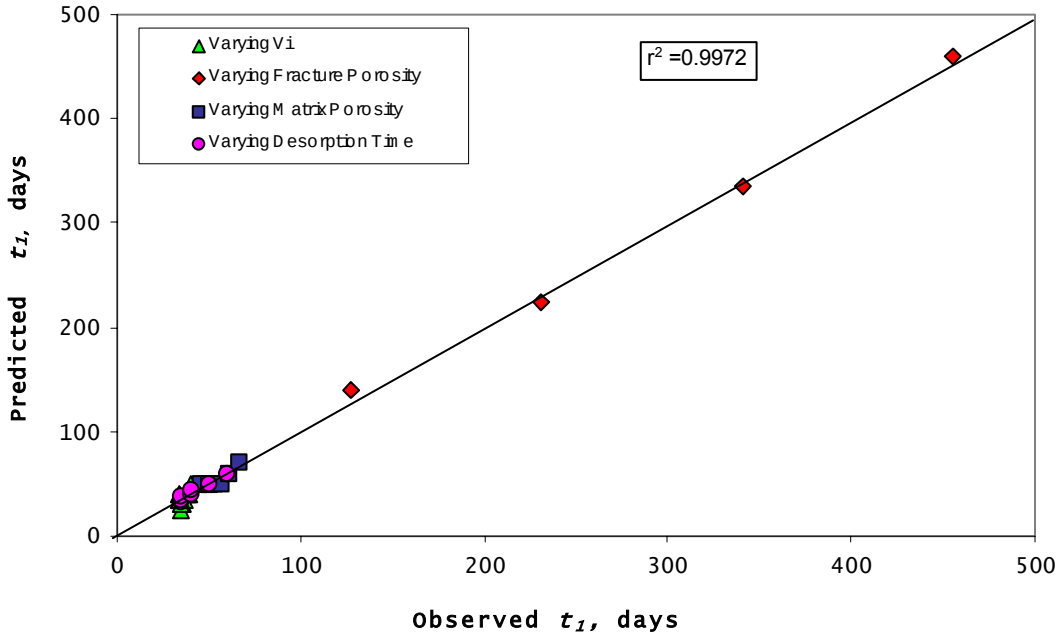

Figure 6.4b- Generalized correlation for t_1 for increased gas rates.

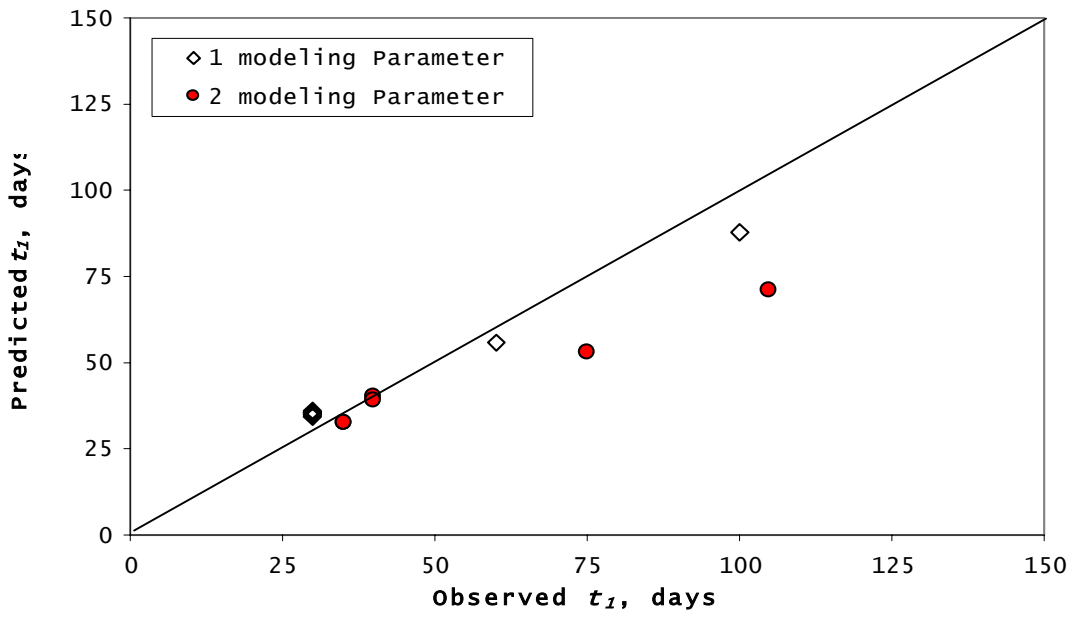

Figure 6.5- New points generated from simulation results to test the correlation equation for t_1. 1 modeling parameter means that just one parameter is being changed from the base case. While 2 modeling parameters means that two different parameters are being changed from the base case.

The t_2, time to 2nd peak was the second parameter variable to be correlated with the modeling variables. Equation 6.3 shows the predictive equation for t_2 and the modeling parameters that were considered for the multiple regression. The parameter group for the correlations consists of only three parameters; initially adsorbed gas (V_i), fracture porosity (ϕ_f) and the matrix porosity (ϕ_m). It was found from simulation results that t_2 is insensitive to desorption time (τ) i.e. the desorption remains constant with changing τ (see **Figure C-6**). For this reason desorption time was not included as a modeling parameter for the regressional correlation to determine the predictive equation.

The correlations for t_2 shown in **Figure 6.6** is a plot of the predicted t_2 (values using the predictive equation) versus observed t_2 (simulation results). To test the predictive equation for t_2, simulation results (observed t_2) are compared to predicted t_2 values which are based on the equation, see **Figure 6.7**. See Table C-2 for simulation test case input data.

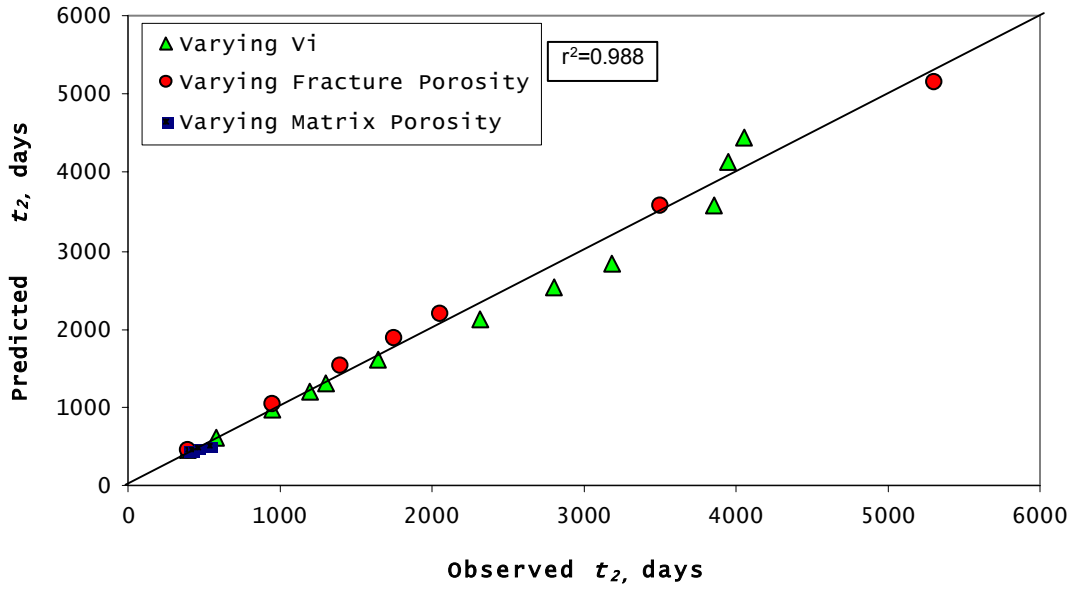

Figure 6.6- Generalized correlation for t_2.

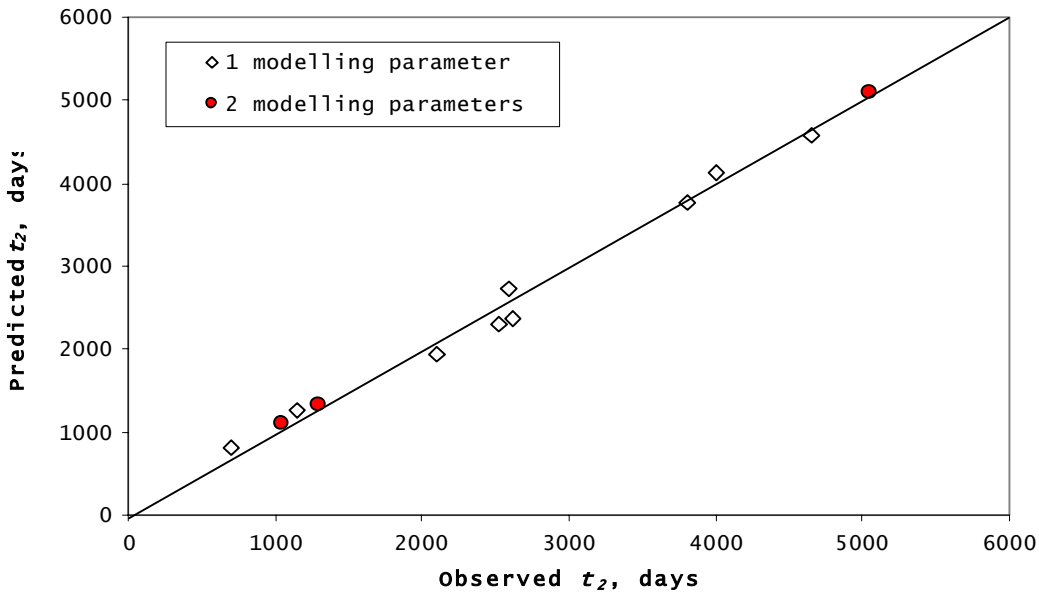

Figure 6.7- New points to test the correlation equation for t_2.

The magnitudes of the peak gas rate, q_1 and q_2 were the next set of parameter variables that were correlated. q_1 represents the peak gas rate at the first peak and q_2 represents the peak gas rate at the second peak. Equation 6.4 and 6.5, shows that all four modeling parameters were considered for the generalized correlations to develop the predictive equations for q_1 and q_2. And the developed equations are able to predict simulation rates within the given range as is shown in **Figure 6.8** & **Figure 6.10.** As was done for the previously discussed correlations the predictive equation is tested with new simulation cases, which will include not only gas rates generated by varying one parameter but also gas rates generated by varying more than one parameter. These results for parameter variables q_1 and q_2 are shown in **Figure 6.9** and **Figure 6.11** and the simulation cases are tabulated in Table C-2.

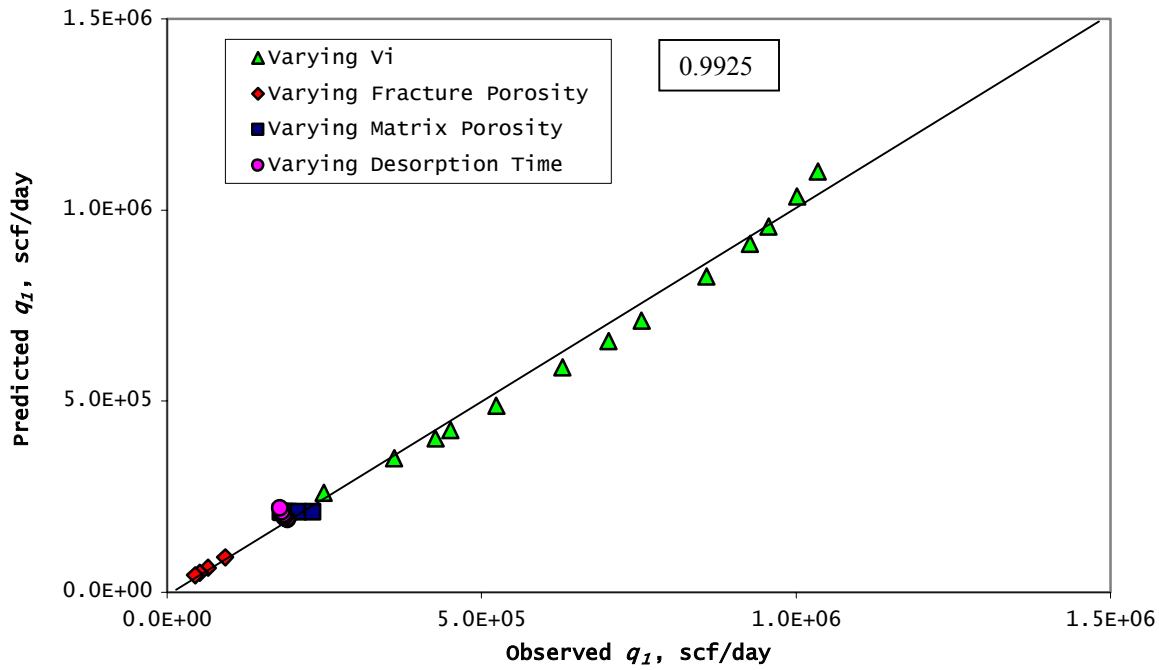

Figure 6.8- Generalized correlation for q_1.

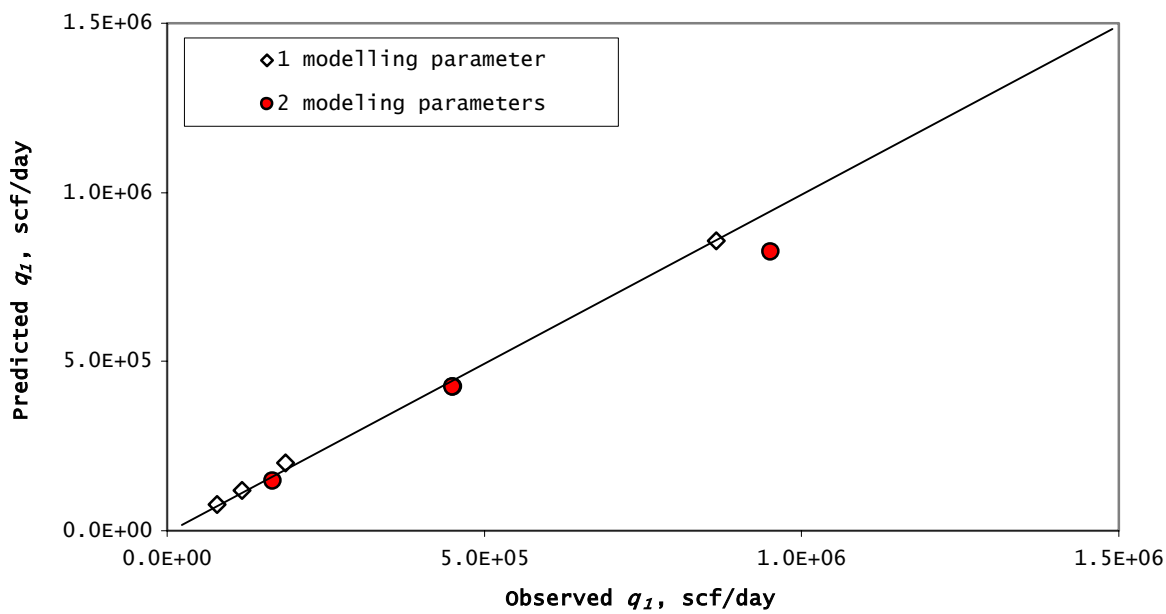

Figure 6.9- New points to test the correlation equation for q_1.

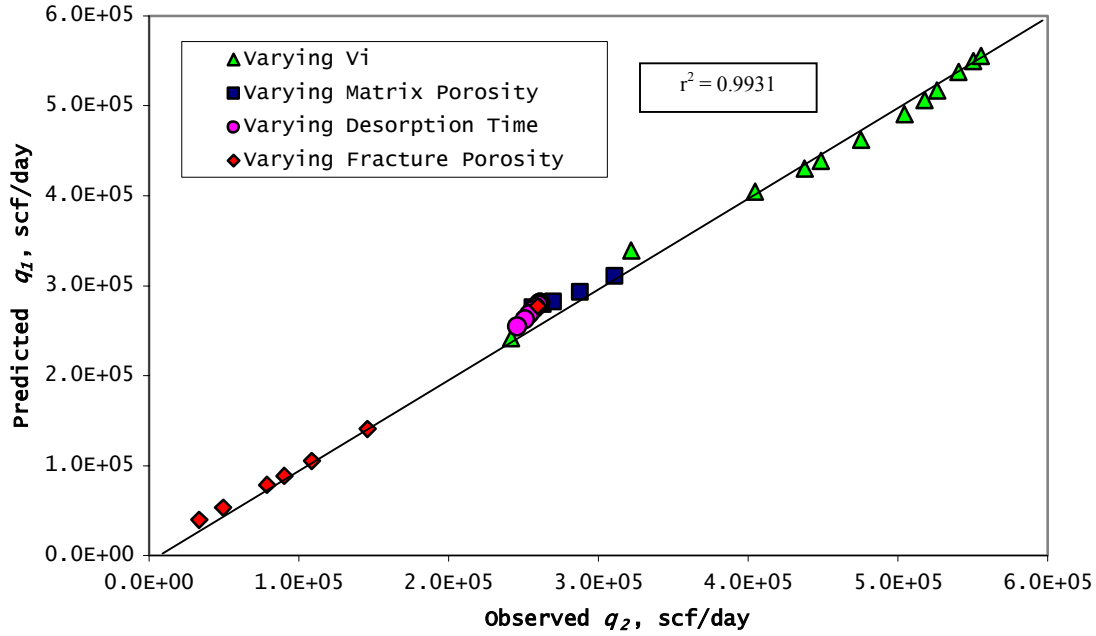

Figure 6.10- Generalized correlation for q_2.

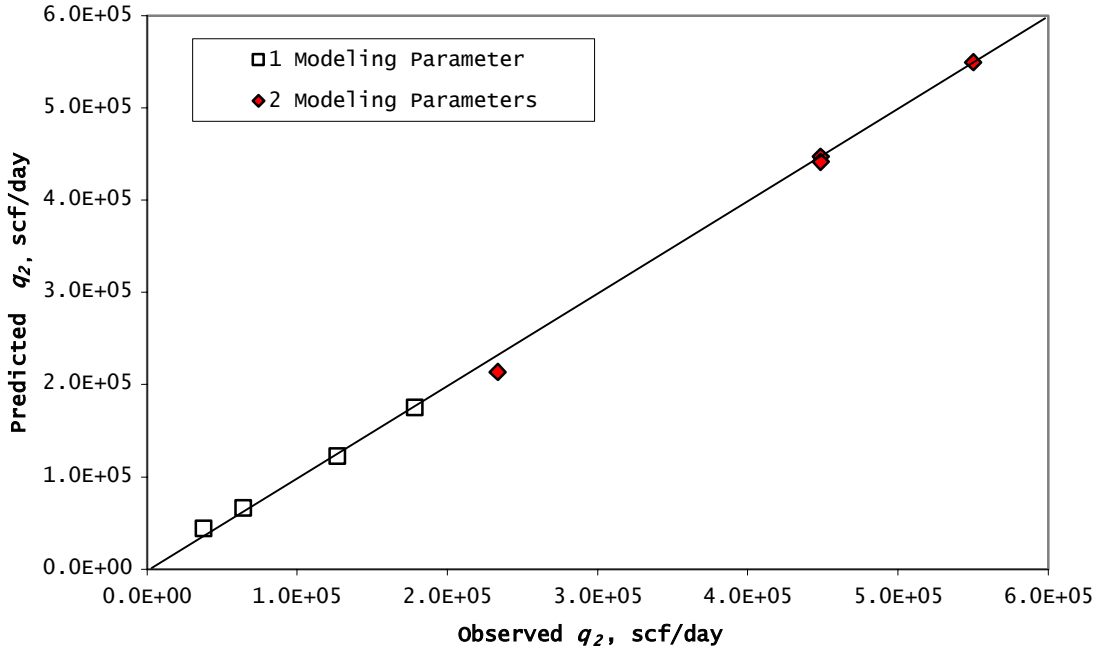

Figure 6.11- New points to test the correlation equation for q_2.

CHAPTER VII
CONCLUSIONS AND RECOMMENDATIONS

7.1 Sensitivity Analysis

1. The desorption time controls the diffusion process and an increase slows down the diffusion process and therefore decreases the gas production rates while increasing the water production rates. The Peak gas rate is also seen to decrease with increase in desorption time.

2. Variations in the matrix permeability does not affect the gas and water production rates, since the flow from the matrix to the fracture is a diffusive process. So the matrix permeability and relative permeability curves defined in CMG are redundant and not actually used for computations.

3. Increasing the fracture system permeability increases the gas and water production rates, and this is simply because the fracture system is the major conduit for flow in coalbed methane reservoirs.

4. Increasing the matrix porosity increases the gas production rates, even through the adsorbed gas volume is decreasing. And increasing the fracture porosity decreases the gas production rates.

5. Reservoirs that are initially saturated have higher gas production rates than

reservoirs that were initially undersaturated. And increase in the initially adsorbed gas volumes will increase the gas production rates and decrease the water production rates.

7.2 Generalized Correlations

1. A set of predictive equations for the dual peaking process was developed and documented. The equations are suitable for determining the magnitude (q_1 and q_2) and times of peak (t_1 and t_2) in a dual peaking gas well.

2. We identified that the dual peak gas rate behavior can be controlled by some simulator input modeling parameters. So for modeling purposes, this behavior which is typically seen in the field can be imitated for history matching purposes by performing sensitivity on these parameters. These modeling parameters include the initially adsorbed gas volume (V_i), desorption time (τ), the fracture porosity (ϕ_f) and the matrix porosity (ϕ_m).

3. From the sensitivity analysis and simple linear correlation, we observe that the fracture porosity does have a significant effect on the peak gas rate and time to peak unlike the matrix porosity which little or no effect.

4. The time to 2nd peak (t_2) in insensitive to the change in desorption time (τ). In other words, for varying desorption time ranging from 0.5-100 days the time to 2nd peak (t_2) remains constant (see Table C-1).

5. Although these correlations have been developed for a specific range of data, the approach and use of parameters can be used in evaluating other field cases.

7.3 Recommendations for Future Work

1. For the sensitivity analysis the fracture permeability should probably be considered. Since we have seen from Appendix D, that this has an effect on the transmissibility of the fractures and therefore affects the gas rates, especially for cases with lots of gas adsorbed.

2. Modeling and comparing different drainage areas (e.g. square and rectangular) would also be useful, to see the effect on the dual peak, while varying different modeling parameters.

3. Incorporating the Palmer Monsoori effect; pressure dependent permeability, into the model would be useful while comparing results from other simulators.

NOMENCLATURE

D = Diffusion coefficient, cm^2/sec or Diffus(k) = Diffusivity constant.

C = Coalbed gas content, Mscf/rcf

CH_4 = Methane

A = Surface area of matrix element, ft^2

$\overline{C}$ = Average gas concentration in the matrix, scf/ft^3.

*** Note that the notations $\overline{C}$ and V both represent the gas content in the matrix.**

V = Gas content in the matrix, scf/ft^3

V_i = Initial gas content in the matrix (at p_i of the matrix)

V_L = Langmuir volume, Mscf / rcf

p_L = Langmuir pressure, psia

Lang = Langmuir

p_f = Coal fracture pressure, psia

q_g = Gas flow rate, scf/day

Vol = Bulk volume, ft^3

τ = Desorption time, days

S_g = Gas saturation, fraction

t_p = Time to peak, days

k_g = Gas permeability

μ_g = Gas viscosity, cp

R_i = Radius of spherical micropore sub element, ft

L = Length, ft

F_s = Shape factor, $1/ft^2$

ϕ = Porosity

ρ = Density, lb/ft^3

t_1 = Time to 1st peak

t_2 = Time to 2nd peak

q_1 = Gas rate at 1st peak

q_2 = Gas rate at 2nd Peak

k_m = Matrix permeability

k_f = Fracture permeability

Subscript

i = initial

g = gas

f = fracture

m = matrix

Units

scf = standard cubic feet

Mscf = 10^6 scf

Bcf = billion cubic feet = 10^9 cubic feet

rcf = reservoir cubic feet

REFERENCES

1. Addington, D.V., "An Approach to Gas-Coning Correlations for a Large Grid Cell Reservoir Simulator," *Journal of Petroleum Technology*, (November 1981), 2267.
2. Remner, D.J., David J., Ertekin, T., Turgay and Sung.: "A Parametric Study of the Effects of Coal Seam Properties on Gas Drainage Efficiency", paper SPE 13366, presented at SPE Eastern Regional Meeting held in Charleston, West Virginia, Oct.30 – Nov.2, 1984.
3. Odusote. O., Ertekin, T., Smith, D. H., Bromhal, G. and Neal Sams,W.: "Carbon Dioxide Sequestration in Coal Seams: A Parametric Study and Development of a Practical Prediction/Screening Tool Using Neuro-Simulation", paper SPE 90055, presented at 2004 SPE Annual Technical Conference and Exhibition held in Houston, Texas, Sept 26-29, 2004.
4. Chaiananansutcharit, T., Chen, H. and Teufel, L.W.: "Impacts of Permeability Anisotropy and Pressure Interference on Coalbed Methane", paper SPE 71069, presented at 2004 SPE Rocky Mountain Petroleum Technology Conference held in Keystone, Colorado, 21-23 May 2001.
5. Cervik, J.: "Behavior of Coal-Gas Reservoir," paper SPE 1973 presented at the SPE 4th Annual Eastern Regional Meeting to held in Pittsburgh, Pennsylvania. Nov 2-3, 1967.
6. Warren, J.E. and Root, P.J.: "The Behavior of Naturally Fractured Reservoirs" paper SPE 426 presented at the Fall Meeting of the Society of Petroleum Engineers in Louisiana. Oct 7-10, 1962.

7. Reeves, S. and Pekot, L.: "Advanced Reservoir Modeling in Desorption-Controlled Reservoirs" paper SPE 71090 presented at the SPE Rocky Mountain Petroleum Technology Conference held in Keystone, Colorado. May 21-23, 2001.
8. Seidle, J.P. and Arri, L.E.: "Use of Conventional Reservoir Models For Coalbed Methane Simulation" paper presented at the International Technical Meeting Jointly hosted by The Petroleum Society CIM and the Society of Petroleum Engineers in Calgary, Alberta Canada. June 10-13, 1990.
9. Thomas, Tan.: "Advanced Large –Scale Coalbed Methane Modeling Using a Conventional Reservoir Simulator" paper presented at the SPE Gas Technology Symposium held in Calgary, Alberta, Canada. 30 April - 2 May, 2002.
10. Paul, G.W., Sawyer, W.K. and Dean, R.H.: "Validation of 3D Coalbed Simulators" paper presented at the 65th Annual Technical Conference and Exhibition of the Society of Petroleum Engineers held in New Orleans, Lousiana. Sept 23-26, 1990.
11. Guo, Xiao, Du, Zhimin. and Shilun, Li.: "Computer Modeling and Simulation of Coalbed Methane Reservoir" paper SPE 84815 presented at the SPE Easter Regional/AAPG Eastern Section Joint Meeting held in Pittsburgh, Pennslyvania. Sept 6-10, 2003.
12. Derickson, J.P., Horne, J.S., Fisher, R.D. and Stevens, S.H.: "Huaibei Coalbed Methane Project, Anhui Province, People's Republic of China", paper SPE 48886 presented at the 1998 SPE International Conference and Exhibition, Beijing, 2-6 November 1998.
13. King, G.R., "Material-Balance Techniques For Coal-Seam and Devonian Shale Gas Reservoirs with Limited Water Influx," SPE Reservoir Engineering, (Feb 1993), 62.

14. Jochen, V.A., Lee, W.J., Semmelbeck, M.E and Jochen. M.E.: " Determining Permeability in Coalbed Methane Reservoirs", paper SPE 28584, presented at 1994 SPE 69th Annual Conference and Exhibition held in New Orleans, Louisiana, Sept 25-28, 1994.

15. Report of Lab Analysis by Ticora Geosciences, INC. Submitted to El Paso Production Company, James Peterson 2-10H, RAPIDGAS Analysis.

16. Roger, N.: "The Langmuir Isotherm", http://www.chem.qmw.ac.uk/surfaces, Feb 2005.

17. Kohler, E.T. and Ertekin, Turgay: "Modeling of Undersaturated Coal Seam Gas Reservoirs", paper SPE 29578 prepared for presentation at SPE Rocky Mountain Regional/Low-Permeability Reservoirs Symposium, Denver, Colorado, Mar 20-22,1995.

18. CMG; GEM 2003.10 User Guide, Computer Modeling Group Calgary, Canada.

19. Zuber, M.D., Sawyer, W.K., Schraufnagel, R.A. and Kuuskraa,V.A.: " The Use of Simulation and History Matching To Determine Critical Coalbed Methane Reservoir Properties", paper presented at the SPE/DOE Low Permeability Reservoir Symposium held in Denver, Colorado. May 18-19,1997.

20. Kazemi, Hossein, Gilman, J.R., and Elsharkawy, A.M.: "Analytical and Numerical Solution of Oil Recovery From Fractured Reservoirs With Empirical Transfer Functions SPE Reservoir Engineering, (May 1992), 219-227.

21. Metcalfe, R.S., Yee, D., Seidle, J.P, and Puri.R: "Review of Research Efforts in Coalbed Methane", paper SPE 23025 prepared for presentation at SPE Asian-Pacific Conference, Perth, Western Australia, Nov 4-7, 1991.

APPENDIX A

CMG BASE CASE DATA FILE

A.1 CMG data file for 80 Acres 21*21*1 Single Well Model

*Note that this the base case shown in Table 5.1. **T**he modeling parameters that were varied for sensitivity and correlations will be in bold italics and notes.

```
RESULTS SIMULATOR GEM
RESULTS SECTION INOUT
*DIM *MAXPERCENT_OF_FULLYIMPLICITBLOCKS 100
*TITLE1  'CBM 80 ACRE 21*21 SINGLE WELL MODEL'
*INUNIT *FIELD

*INTERRUPT *INTERACTIVE
*RANGECHECK *ON
*XDR *ON
*MAXERROR  20
*WRST 0
*WPRN *WELL  1
*WPRN *GRID  *TIME
*WSRF *WELL 1
*WSRF *GRID 1
*OUTPRN *WELL *ALL
*OUTPRN *GRID PRES SW SG DENW DENG VISG ADS 'C1' Y 'C1'
*OUTPRN *RES *ALL
*OUTSRF *GRID PRES SW SG DENW DENG VISG ADS 'C1' Y 'C1'
*OUTSRF *RES *ALL

GRID CART 21 21 1
KDIR DOWN
*DI *IVAR 46.66904756 19*93.33809512 46.66904756
*DJ *JVAR 46.66904756 19*93.33809512 46.66904756
DK CON 30

PAYDEPTH ALL
```

```
        441*3280.84
DUALPOR
**FRACTURE AND MATRIX POROSITY
POR MATRIX CON 0.005
POR FRACTURE CON 0.001

**FRACTURE AND MATRIX PERMEABILITIES
PERMI MATRIX CON 0.0001      **k_m = 0.001 md
PERMI FRACTURE CON 2         **k_f = 2 md
PERMJ MATRIX CON 0.0001
PERMJ FRACTURE CON 2
PERMK MATRIX CON 0.0001
PERMK FRACTURE CON 2

**FRACTURE SPACING
DIFRAC CON 0.042
DJFRAC CON 0.042
DKFRAC CON 0.042

**FRACTURE AND MATRIX PORE COMPRESSIBILITIES
CPOR  MATRIX   100E-06
PRPOR MATRIX  1109.54
CPOR  FRACTURE 100E-06
PRPOR FRACTURE 1109.54

**METHANE GAS PROPERTIES
RESULTS SECTION VOLMOD
RESULTS SECTION SECTORLEASE
RESULTS SECTION ROCKCOMPACTION
RESULTS SECTION GRIDOTHER
RESULTS SECTION MODEL
*MODEL       *PR
*NC          1  1
*COMPNAME    'C1'
*HCFLAG      0
*VISCOR      *HZYT
*VISCOEFF    0.1023
```

```
        0.023364
        0.058533
        -0.040758
        0.0093324
*MIXVC      1
*TRES       113.**F
*PCRIT      45.400000
*TCRIT      190.60000
*AC         0.008000
*VCRIT      0.099000
*MW         16.04300
*PCHOR      77.00000
*SG         0.300000
*TB         -258.61000
*VISVC      0.099000
*VSHIFT     0.000000
*OMEGA      .457235530
*OMEGB      .077796074
**PVC3      1.2
*PHASEID    *DEN
**BIN
**    0.103
*DENW       62.4
*CW         3.99896E-06
*REFPW      14.69595
*VISW       0.607

RESULTS SECTION MODELARRAYS
RESULTS SECTION ROCKFLUID


**-------------------------------------------------ROCK FLUID----------
*ROCKFLUID
*RPT 1  *DRAINAGE
**RELATIVE PERMEABILITY DATA FOR THE MATRIX
*SWT
**   Sw       Krw       Krow
```

0.000000 0.000000 0.000010 0.000000
0.050000 0.000600 0.0000095 0.000000
0.100000 0.001300 0.000009 0.000000
0.150000 0.002000 0.0000085 0.000000
0.200000 0.007000 0.000008 0.000000
0.250000 0.015000 0.0000075 0.000000
0.300000 0.024000 0.000007 0.000000
0.350000 0.035000 0.0000065 0.000000
0.400000 0.049000 0.000006 0.000000
0.450000 0.067000 0.0000055 0.000000
0.500000 0.088000 0.000005 0.000000
0.550000 0.116000 0.0000045 0.000000
0.600000 0.154000 0.000004 0.000000
0.650000 0.200000 0.0000035 0.000000
0.700000 0.251000 0.000003 0.000000
0.750000 0.312000 0.0000025 0.000000
0.800000 0.392000 0.000002 0.000000
0.850000 0.490000 0.0000015 0.000000
0.900000 0.601000 0.000001 0.000000
0.950000 0.731000 0.0000005 0.000000
0.975000 0.814000 0.00000025 0.000000
1.000000 1.000000 0.000000 0.000000

*SLT
** Sl Krg Krog
0.000000 1.000000 0.000000 0.000000
0.050000 0.835000 0.0000005 0.000000
0.100000 0.720000 0.000001 0.000000
0.150000 0.627000 0.0000015 0.000000
0.200000 0.537000 0.000002 0.000000
0.250000 0.466000 0.0000025 0.000000
0.300000 0.401000 0.000003 0.000000
0.350000 0.342000 0.0000035 0.000000
0.400000 0.295000 0.000004 0.000000
0.450000 0.253000 0.0000045 0.000000
0.500000 0.216000 0.000005 0.000000
0.550000 0.180000 0.0000055 0.000000

```
0.600000  0.147000  0.000006  0.000000
0.650000  0.118000  0.0000065  0.000000
0.700000  0.090000  0.000007  0.000000
0.750000  0.070000  0.0000075  0.000000
0.800000  0.051000  0.000008  0.000000
0.850000  0.033000  0.0000085  0.000000
0.900000  0.018000  0.000009  0.000000
0.950000  0.007000  0.0000095  0.000000
0.975000  0.003500  0.00000975  0.000000
1.000000  0.000000  0.000010  0.000000

*RPT 2  *DRAINAGE
*SWT
**RELATIVE PERMEABILITIES FOR THE FRACTURE.
0.000000  0.000000  1.000000  0.000000
1.000000  1.000000  0.000000  0.000000

*SGT
0.010000  0.000000  1.000000  0.000000
1.000000  1.000000  0.000000  0.000000

*KROIL *STONE2 *SWSG
RTYPE MATRIX CON 1.
RTYPE FRACTURE CON 2.

**FRACTURE AND MATRIX DENSITIES
ROCKDEN MATRIX CON 89.5841
ROCKDEN FRACTURE CON 89.5841
**METHANE ADSORPTION DATA
**ADGMAXC -Maximum moles of adsorbed gas per unit mass of rock (gmol/lb of rock)
**ADGCSTC -A constant the represents the inverse of the langmuir pressure pL (1/Psia)
```

****ADGMAXC 'C1' *MATRIX *CON 0.2268*** **** V_L = 0.2268 gmol/lb of rock**

****ADGCSTC 'C1' *MATRIX *CON 0.00137895*** **** p_L = 0.00137895 1/psia**

```
*ADGMAXC 'C1' *FRACTURE  *CON 0
*ADGCSTC 'C1' *FRACTURE  *CON 0
```

```
**DESORPTION TIME, τ
COAL-DIF-TIME 'C1' MATRIX CON 10    ** τ = 10 day

**INITIAL CONDITION
*INITIAL
*VERTICAL *OFF
*PRES *MATRIX      *CON 725.189  **p_m = 725.189 psia
*PRES *FRACTURE    *CON 1109.54  **p_f = 1109.54 psia
*SW *MATRIX        *CON 0.00001
*SW *FRACTURE      *CON 0.9999
*ZGLOBAL *MATRIX    *CON 10
*ZGLOBAL *FRACTURE  *CON 10

**NUMERICAL
*NUMERICAL
*DTMAX 365.
*DTMIN 0.01
*CONVERGE *PRESS 0.514884

**WELL DATA
RUN
DATE 2000 01 01
DTWELL 1.E-06
*DTMIN 1.E-07
AIMSET FRACTURE CON 3.
AIMSET MATRIX CON 3.

WELL  1 'PRODUCER'
PRODUCER 'PRODUCER'
OPERATE MAX STW 512.57962 CONT
OPERATE MIN BHP 50 CONT
GEOMETRY K 0.11975 0.249 1. 0.
PERF GEO   'PRODUCER'
          11 11 1 1. OPEN FLOW-TO 'SURFACE'
TIME 1
TIME 3
TIME 5
```

TIME 10

TIME 15

.

TIME 1500

.

TIME 3000

.

TIME 4350

.

TIME 6050

.

TIME 8000

STOP

********** TERMINATE SIMULATION **********

APPENDIX B

DESORPTION TIME AND RATE EQUATIONS FOR COALBED METHANE

Cervik, J., SPE 1973

Fick' s Law of Diffusion; $q' = -DA\frac{dc}{dL}$ ……..(.B-1)

Where; D, Diffusion Coefficient = cm^2/sec

C, Concentration = ft3/lb of coal

Paul,G.W., SPE 20733

Rate at which gas enters into the cleat system; $-\frac{dC}{dt} = (\frac{1}{\tau})(C - C_w)$ ……....(B-2)

Where; C, Concentration = Mcf/rcf reservoir

τ , Sorption time = days

Zuber, et al., SPE 16420

Desorption Time; $\tau = \frac{s^2}{D*8*\pi}$ ……(B-3)

Flow rate from Matrix to Fracture; $q_m(p) = \alpha A_{sm} D N_e(\overline{C}_{gm} - C_{gm}(p))$ ……..(B-4)

Where; τ , Desorption time = days

s, Cleat Spacing = ft

D, Diffusion Coefficient = ft^2/day

q_m , Flow rate = Scf/day

α , Shape factor (Cylinderical matrix)= ft^{-1}

A_{sm}, Surface area of matrix elements = ft^2

N_e, Number of Matrix Elements = Dimensionless

C, Concentration = Scf/ ft^3

Ticora Geosciences. INC

Desorption Time; $\tau = \dfrac{1}{3600 * \alpha * \dfrac{D}{r^2}}$ …… …….....(B-5)

Where; τ , sorption time = hours

α , Shape factor = cm^2 * Does not seem correct, should be Dimensionless

D, Diffusion Coefficient = cm^2/sec

r^2, Average Diffusion Distance = cm^2

$\dfrac{D}{r^2}$, Diffusivity = sec^{-1}

CMG Simulator

Flow rate from Matrix to Fracture;

$$Rate_{block-basis} = Vol * 4 * \sum (1/FracSpacin\ g)^2 * Diffus(k) * S_g^{A-\mathrm{mod}} (C(k, gas, m) - C(k, gas, f)) \quad \text{...(B-6)}$$

Desorption Time; $\tau = \dfrac{1}{4 * \sum (1/FracSpacing)^2 * D}$ ……..…….(B-7)

Where; Vol, Block Volume = ft^3

Frac Spacing = ft

τ , Desorption time = days

D, Diffusion Coefficient = cm^2/sec

$S_g^{A-\mathrm{mod}}$, Gas saturation in the matrix = Dimensionless = 1

$Rate_{block-basis}$ Flow rate = Scf/day

C, Concentration = gmole/ lb of rock

Dimensional Analysis

Fick' s Law (SPE 1973); $q' = -DA\dfrac{dc}{dL}$ ……..(B-8)

$$= q'\left[\frac{ft^3}{day}\right] = -D\left[\frac{ft^2}{day}\right] * A\left[ft^2\right] * \frac{dC}{dL}\left[\frac{Scf}{ft^3} * \frac{1}{ft}\right]$$

Paul (SPE 20733); $-\dfrac{dC}{dt} = (\dfrac{1}{\tau})(C - C_w)$ ……..……(B-9)

$$-\frac{dC}{dt}\left[\frac{Scf}{ft^3} * \frac{1}{day}\right] = \frac{1}{\tau}\left[\frac{1}{day}\right] * C - C_w\left[\frac{Scf}{ft^3}\right]$$

Multiplying through by the Bulk volume;

$$-\frac{dC}{dt}\left[\frac{Scf}{ft^3} * \frac{1}{day}\right] * Vol\left[ft^3\right] = \frac{1}{\tau}\left[\frac{1}{day}\right] * C - C_w\left[\frac{Scf}{ft^3}\right] * Vol\left[ft^3\right]$$

mass flow rate (ft^3/day) to fracture;

$$-q\left[\frac{Scf}{day}\right] = \frac{1}{\tau}\left[\frac{1}{day}\right] * C - C_w\left[\frac{Scf}{ft^3}\right] * Vol\left[ft^3\right]$$

Zuber et al., (SPE 16420);

$$q_m(p)\left[\frac{Scf}{day}\right] = \alpha\left[\frac{1}{ft}\right] * A_{sm}\left[ft^2\right] * D\left[\frac{ft^2}{day}\right] * N_e * (\overline{C}_{gm} - C_{gm}(p))\left[\frac{Scf}{ft^3}\right] \text{……(B-10)}$$

CMG;

$$Rate_{block-basis}\left[\frac{ft^3}{day}\right] = Vol\left[ft^3\right] * 4 * \Sigma(1/FracSpacing)^2\left[\frac{1}{ft^2}\right] * Diffus(k)\left[\frac{ft^2}{day}\right] * S_g^{A-\text{mod}} * (C(m) - C(f))\left[\frac{SCF}{ft^3}\right]$$

……(B-11)

Desorption Time

Ticora[17] defines the desorption time as the time required to desorb 63.2% of the original gas content if a sample is maintained at constant temperature[17]. The derivation behind this definition starts from the simple diffusion equation and is as follows;

$$\frac{dC}{dt} = -\frac{1}{\tau}\left[\overline{C} - C(p_f)\right] \quad \text{(B-12)}$$

Bringing like terms together and integrating we have that;

$$\int_{c_i}^{c} \frac{dC}{\overline{C} - C(p_f)} = -\frac{1}{\tau}\int_0^t dt \quad \text{(B-13)}$$

$$LN \quad \frac{\overline{C} - C(p_f)}{\overline{C}_i - C(p_f)} = -\frac{1}{\tau}t \quad \text{(B-14)}$$

$$\frac{\overline{C} - C(p_f)}{\overline{C}_i - C(p_f)} = e^{-\frac{1}{\tau}t} \quad \text{(B-15)}$$

Let $C(p_f) = 0$ and t = τ ……(B-16)

$$\frac{\overline{C}}{\overline{C}_i} = e^{-1} = \frac{1}{e} \quad \text{(B-17)}$$

$$\frac{\overline{C}}{\overline{C}_i} = e^{-1} = \frac{1}{e} = 0.3679 \text{ or } 36.79\% \text{ gas is left in the matrix} \quad \text{(B-18)}$$

Amount drained from the matrix @ t=τ becomes;

$$\frac{\overline{C}_i - \overline{C}}{\overline{C}_i} = 1 - \frac{1}{e} = 0.6321 \text{ or } 63.21\% \quad \text{(B-19)}$$

APPENDIX C

CORRELATION DATA AND REGRESSIONAL ANALYSIS PLOTS

For data needed to perform the simple and multiple regression analysis a total of 39 simulation cases of different values of the modeling parameters were run, to determine the time to 1st peak (t_1), magnitude of the 1st peak (q_1), time to 2nd peak (t_2) and magnitude of the 2nd peak (q_2). The simulation results are tabulated below.

Table C-1- Correlation sample data

	Time to Peak, t		Magnitude of Peak, q	
V_1	t_1	t_2	q_1	q_2
0.85	50	400	183,306	259,423
8.5	50	580	249,232	321,908
18.7	50	950	360,973	404,550
56	40	1200	426,566	437,869
112	40	1300	450,584	448,653
187	35	1650	523,485	475,462
374	30	2320	628,682	504,486
560	30	2800	702,146	517,958
747	25	3180	754,520	526,253
1307	30	3850	857,557	540,544
1867	35	3950	926,797	550,333
2241	35	4050	956,380	555,643
2988	40	-	1,001,630	-
3735	40	-	1,034,760	-
τ				
0.5	35	400	191,806	261,457
1	35	400	190,817	261,377
3	35	400	187,350	260,872
5	40	400	186,992	260,467
7	40	400	186,174	259,976
10	50	400	183,306	259,425
15	60	400	179,562	258,329
25	-	400	-	256,082
35	-	400	-	253,906
50	-	400	-	250,842
75	-	400	-	246,124

Table C-1 (CONTINUED)				
v_i	t_1	t_2	q_1	q_2
100	-	400	-	241,729
$\varnothing_f$				
0.001	50	400	183,306	259,425
0.005	140	950	92,357	145,836
0.01	225	1400	65,021	108,640
0.015	335	1750	52,253	90,223
0.02	460	2050	44,513	78,593
0.05	-	3500	-	49,328
0.1	-	5300	-	33,283
$\varnothing_m$				
0.001	50	400	180,420	256,377
0.005	50	400	183,306	259,425
0.01	50	400	186,779	262,966
0.02	50	420	193,574	269,777
0.05	60	460	209,767	287,653
0.1	70	540	232,027	310,849

Simple Regressional Analysis

Prior to developing the generalized correlations each of the modeling parameters have been varied independently to determine its effect on t_1, q_1, t_2 and q_2 using a simple regressional analysis. The simple regressional analysis will show the effect of each modeling parameter on t_1, q_1, t_2 and q_2. The results from these regressional analysis are shown in the following figures;

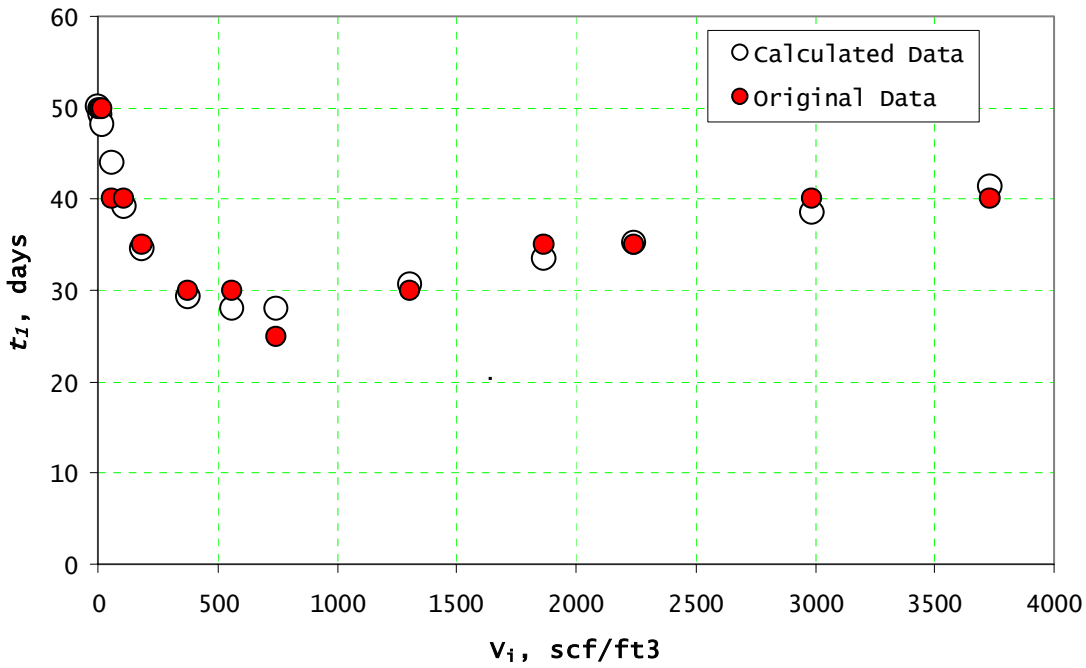

Figure C-1- Simple regression analysis plot showing the linear relationship between t_1 and the initially adsorbed gas volume, V_i.

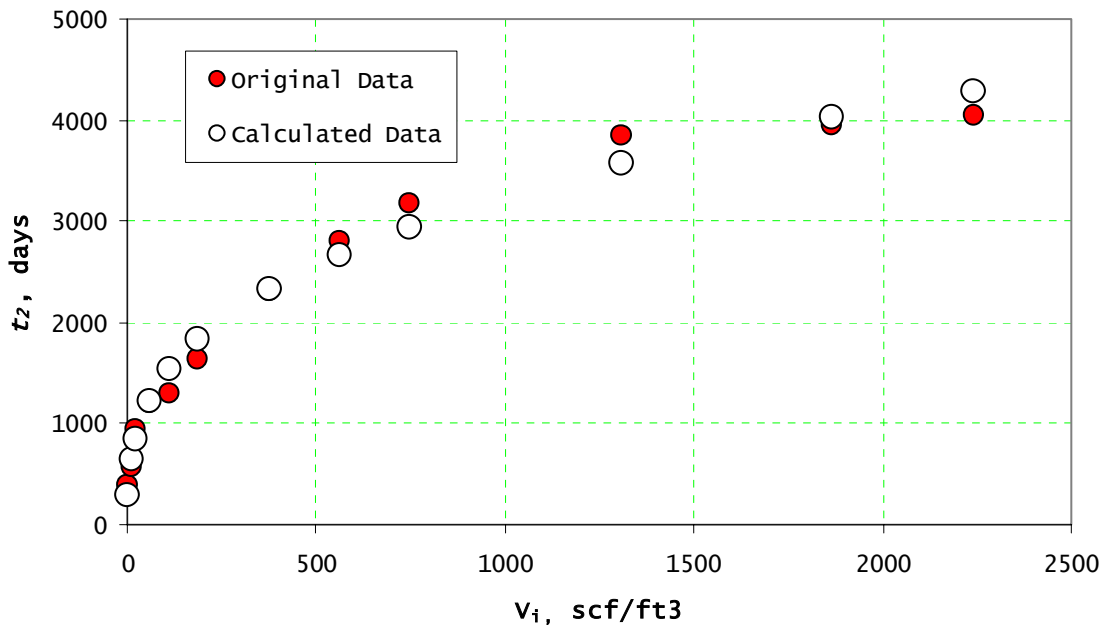

Figure C-2- Simple regression analysis plot showing the linear relationship between t_2 and the initially adsorbed gas volume, V_i.

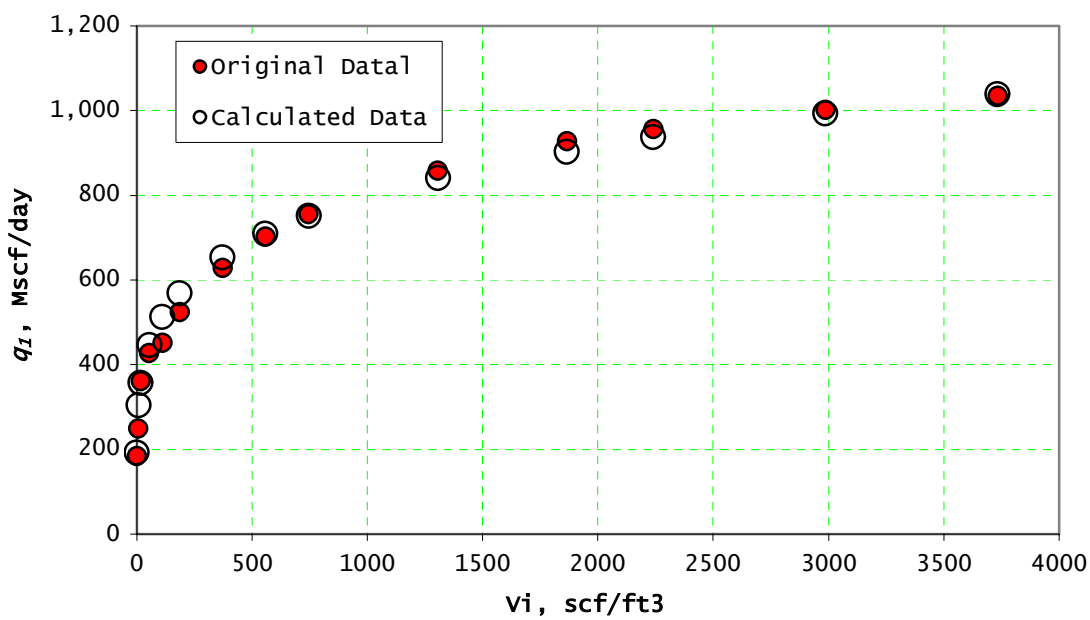

Figure C-3. Simple regression analysis plot showing the linear relationship between q_1 and the initially adsorbed gas volume, V_i.

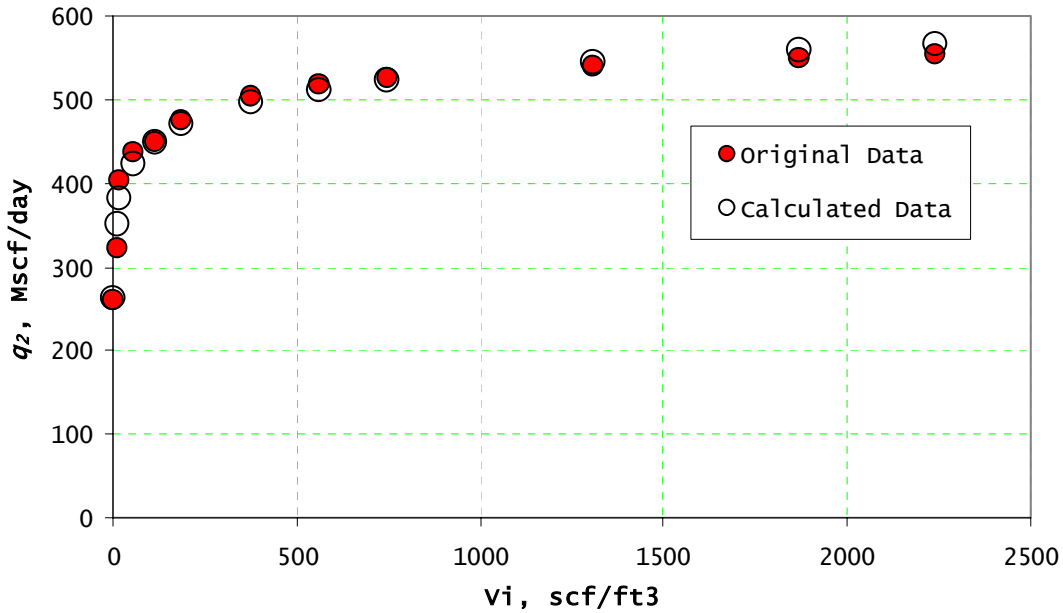

Figure C-4- Simple regression analysis plot showing the linear relationship between q_2 and the initially adsorbed gas volume, V_i.

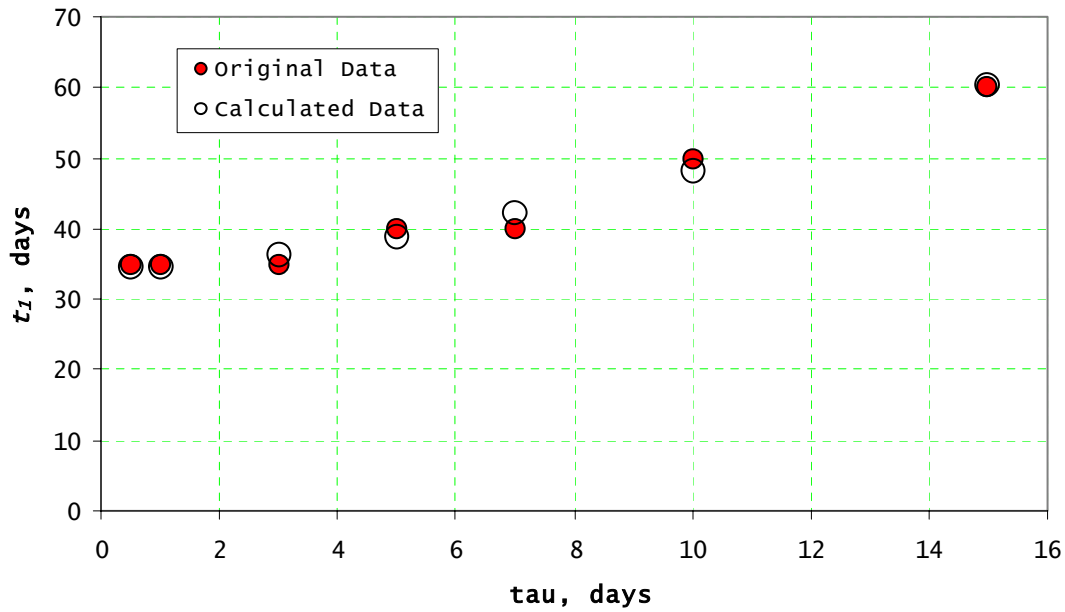

Figure C-5- Simple regression analysis plot showing the linear relationship between t_1 and the desorption time, τ.

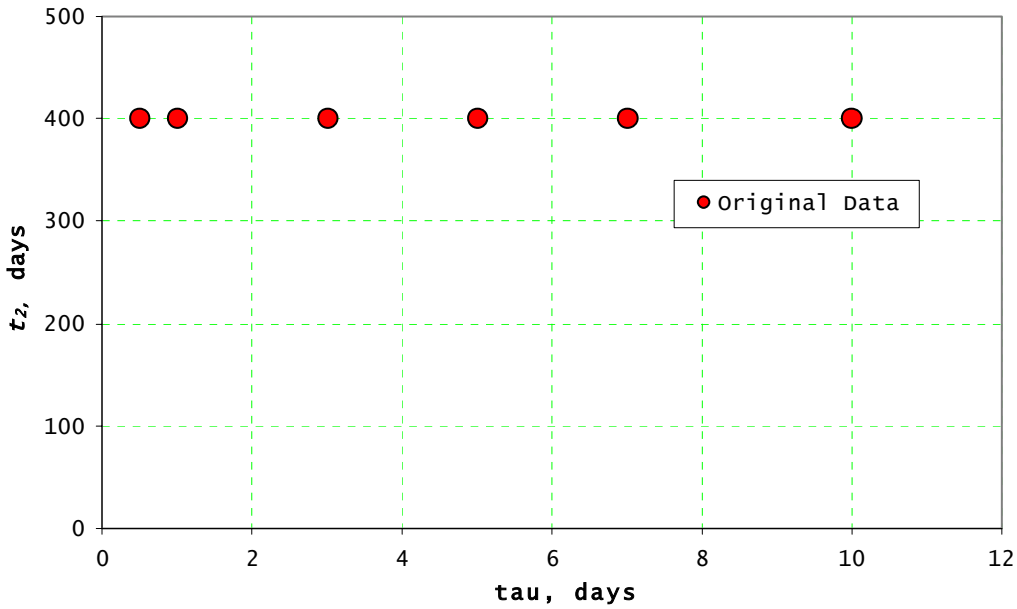

Figure C-6- Simple regression analysis plot showing the linear relationship between t_2 and the desorption time, τ.

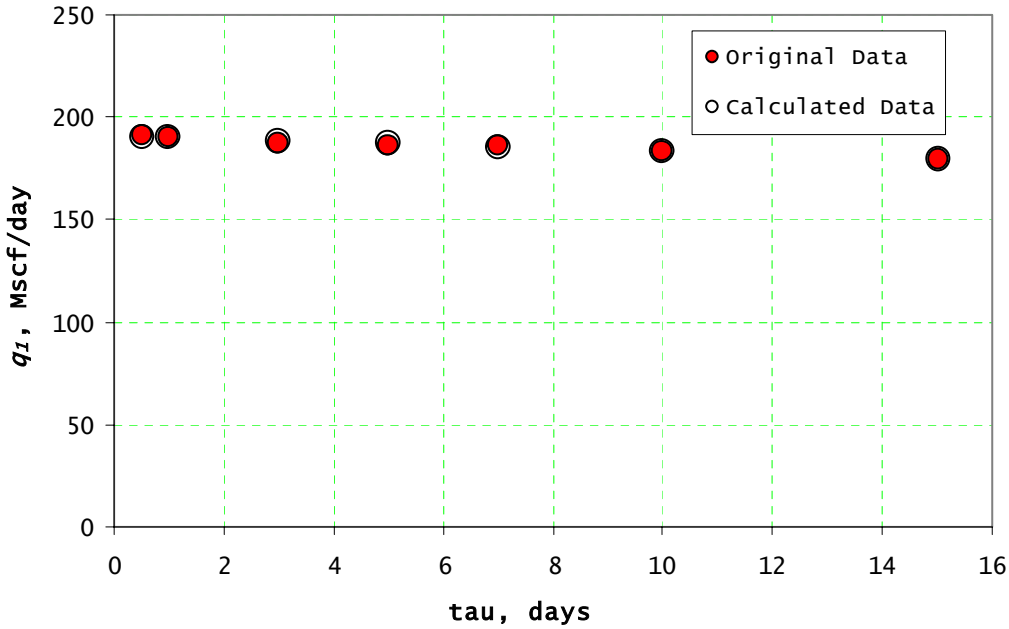

Figure C-7- Simple regression analysis plot showing the linear relationship between q_1 and the desorption time, τ.

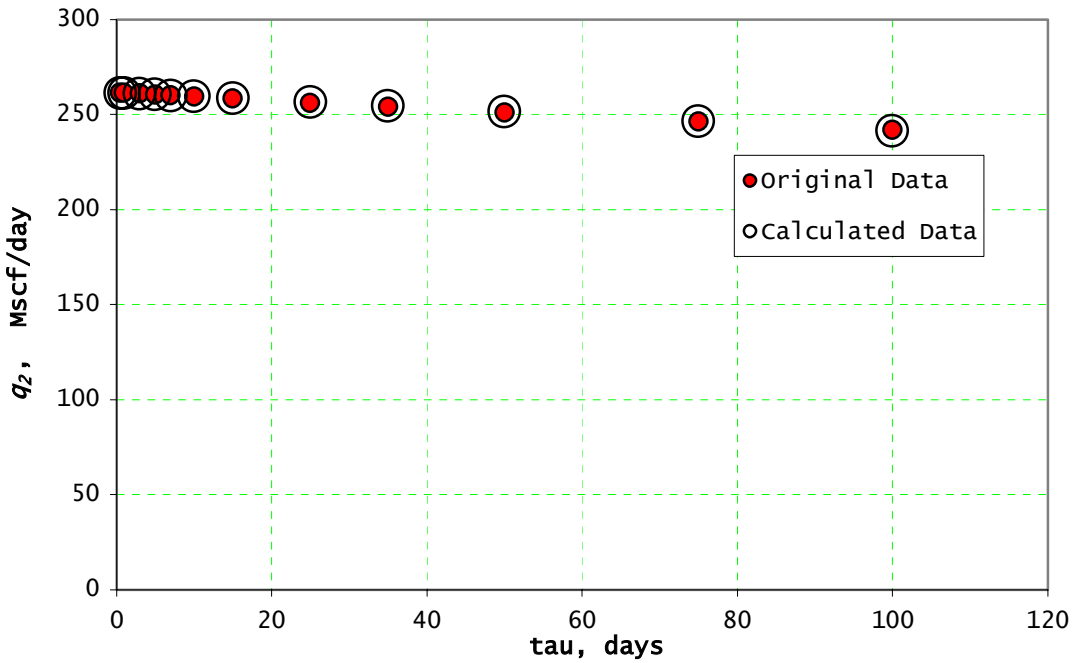

Figure C-8- Simple regression analysis plot showing the linear relationship between q_2 and the desorption time, τ.

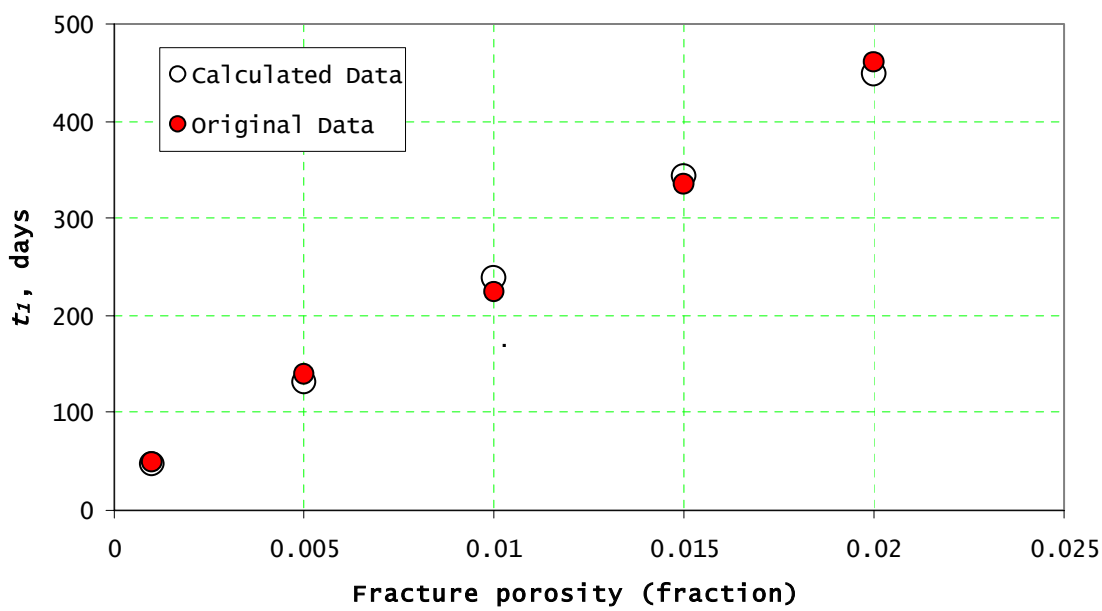

Figure C-9- Simple regression analysis plot showing the linear relationship between t_1 and the fracture porosity, $\varnothing_f$.

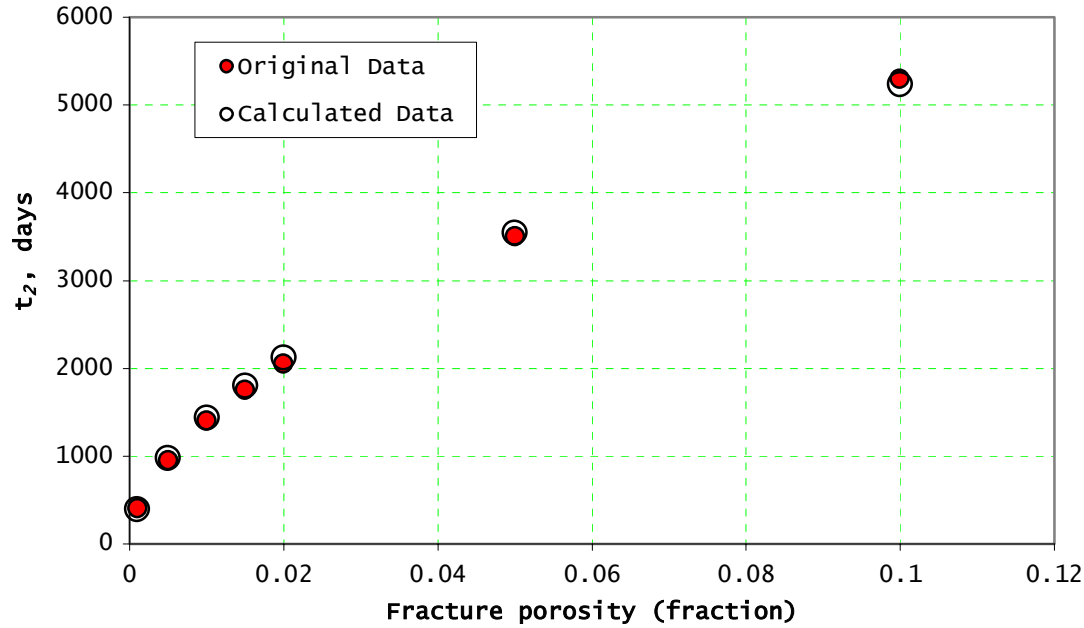

Figure C-10- Simple regression analysis plot showing the linear relationship between t_2 and the fracture porosity, $\varnothing_f$.

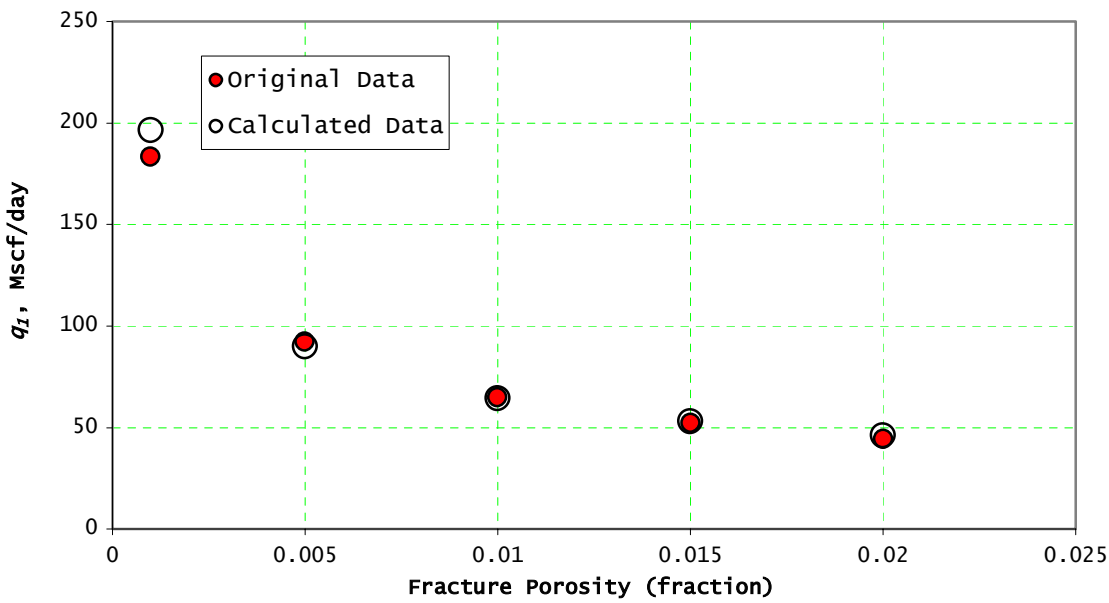

Figure C-11- Simple regression analysis plot showing the linear relationship between q_1 and the fracture porosity, $\varnothing_f$.

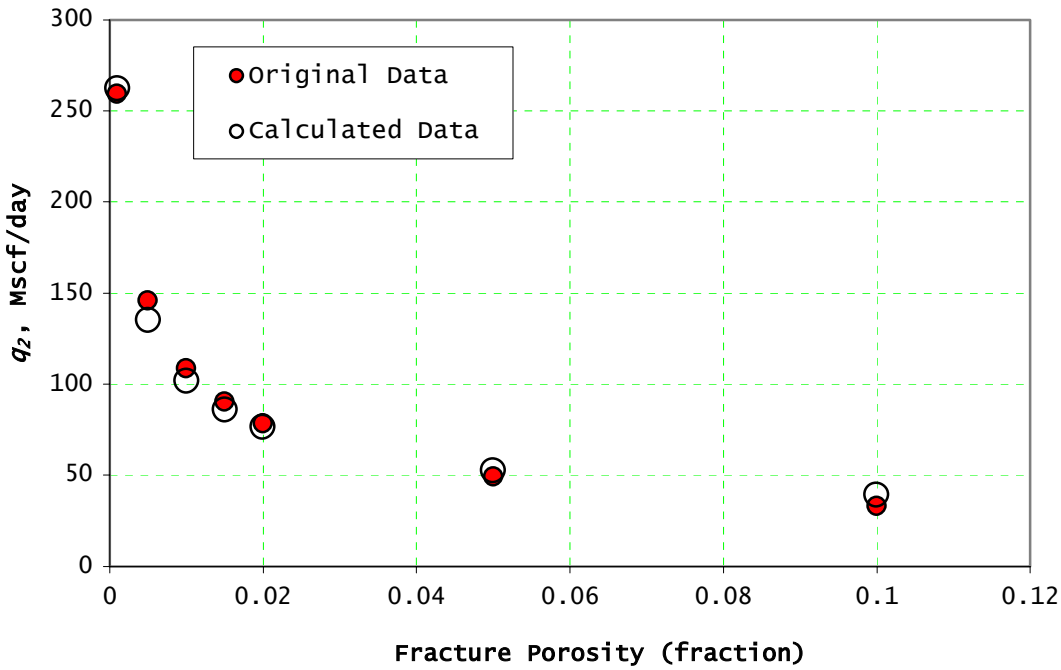

Figure C-12- Simple regression analysis plot showing the linear relationship between q_2 and the fracture porosity, $\varnothing_f$.

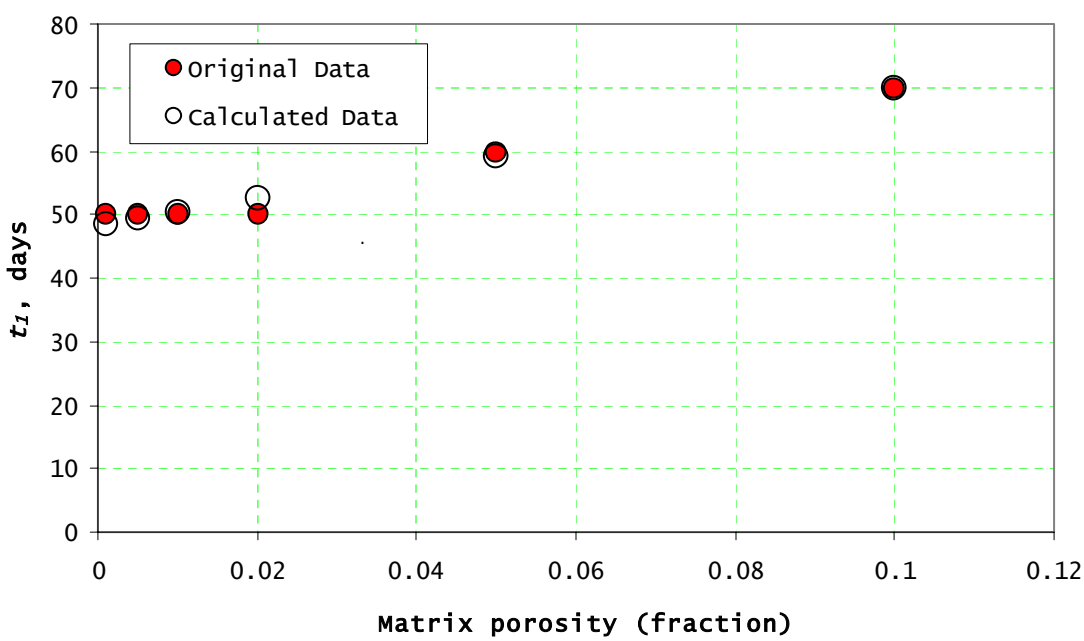

Figure C-13- Simple regression analysis plot showing the linear relationship between t_1 and the matrix porosity, $\varnothing_m$.

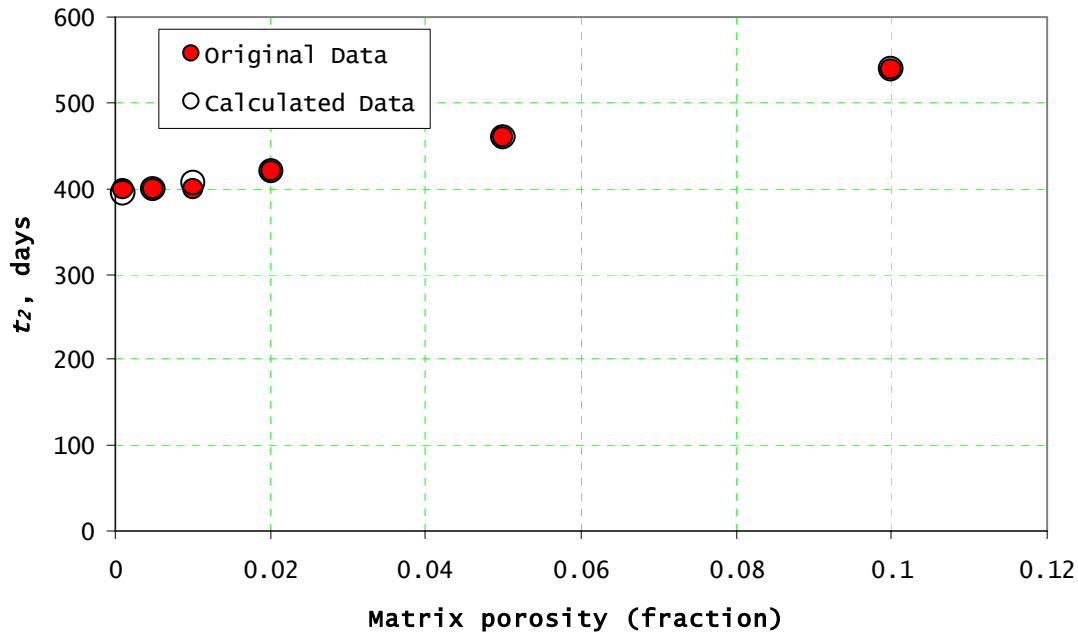

Figure C-14- Simple regression analysis plot showing the linear relationship between t_2 and the matrix porosity, $\varnothing_m$.

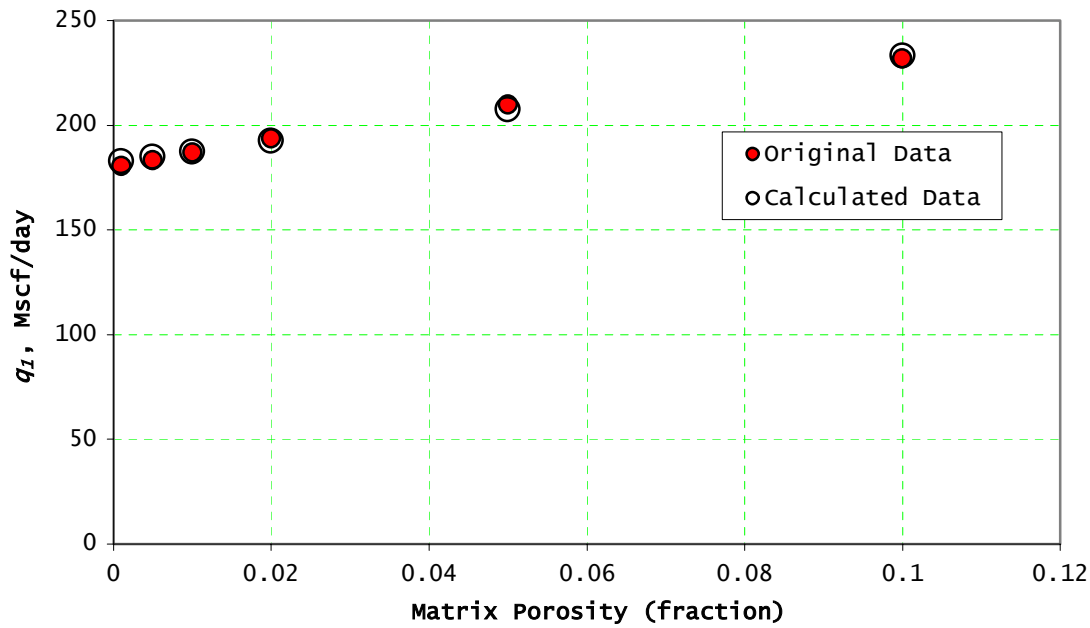

Figure C-15- Simple regression analysis plot showing the linear relationship between q_1 and matrix porosity, $\varnothing_m$.

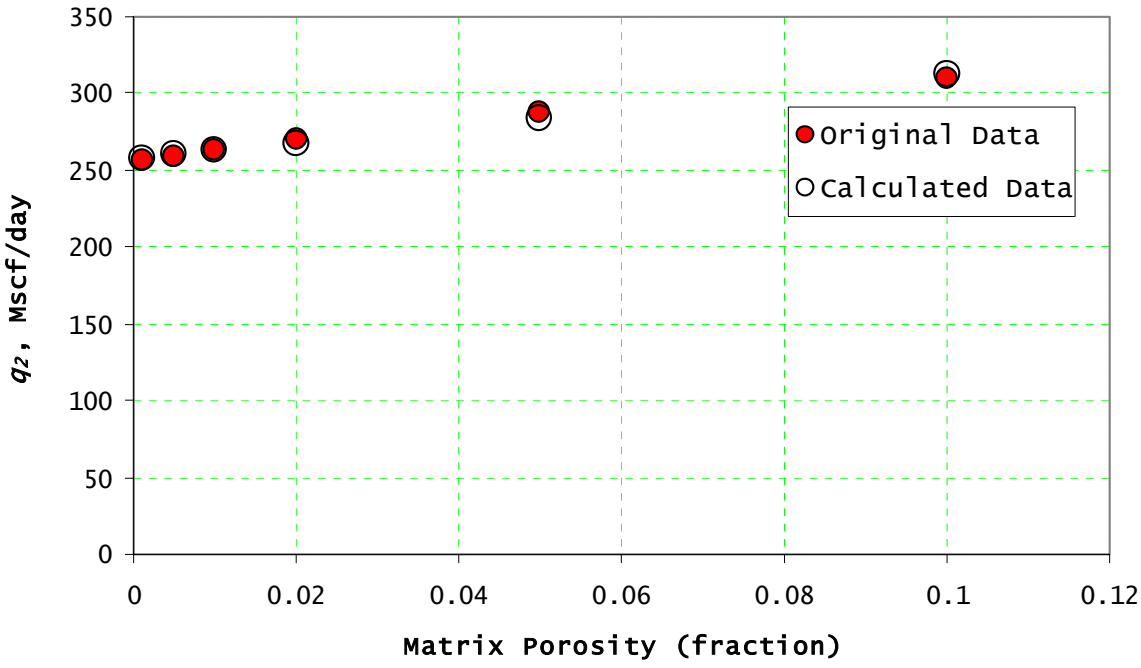

Figure C-16- Simple regression analysis plot showing the linear relationship between q_2 and matrix porosity, $\varnothing_m$.

Simulation Test Results

To test the predictive equations for q_1, q_2, t_1 and t_2, 19 simulation cases were run. The simulation input data and results are tabulated below.

Table C-2 - Simulation cases							
τ	v_i	ϕ_f	ϕ_m	t_1	t_2	q_1	q_2
				(days)	(days)	(scf/day)	(scf/day)
10	1494	0.001	0.005	30	3800	865,598	-
10	299	0.001	0.02	30	2100	-	-
10	448	0.001	0.005	30	2520	-	-
10	933	0.001	0.005	30	-	-	-
10	485	0.001	0.005	30	2620	-	-
13	8.5	0.001	0.005	60	-	-	-
10	8.5	0.003	0.005	100	700	117,479	178,234
10	8.5	0.001	0.005	220	1150	78,892	126,787
10	560	0.001	0.005	75	-	-	-
10	112	0.001	0.005	40	-	449,935	448,472
0.5	1867	0.001	0.005	35	1300	951,761	-
10	112	0.001	0.01	40	-	450,349	448,596
10	18.7	0.003	0.005	105	1050	166,234	233,531
0.5	747	0.001	0.02	35	-	-	-
10	8.5	0.03	0.005	-	2588	-	64,395
10	8.5	0.001	0.005	-	4650	-	37,840
10	1867	0.001	0.005	-	4000	-	550,129
10	93.37	0.015	0.01	-	5050	-	-
5	8.5	0.001	0.005	-	-	186,992	-

APPENDIX D

DESCRIPTION OF THE EFFECT OF FRACTURE AND MATRIX PRESSURES ON GAS RATES

The gas rate sensitivity plots shown in **Figures 5.12** and **5.14** for varying V_i does not show a proportional change in gas rate with the change in the V_i values. For example the case of V_i =18.7 scf/ft^3 gives a q_2 = 360,973 scf/day while another case of V_i =187 scf/ft^3 gives a q_2 = 523,485 scf/day, which has twice as much gas adsorbed as the first case does not have twice as much gas rate. This is simply because for cases where you have a lot of gas adsorbed, the gas rate is dependent on the fracture transmissibility which is a function of the fracture permeability k_f . So for the cases I ran in this study because the base case k_f is 2 md the gas rates through the fractures are not as high as it would be if the k_f is increased.

Figure D-1 shows higher fracture and matrix average pressures for high V_i cases than the lower V_i cases after the start of desorption. And this is because the gas is not flowing out of the fractures as fast as it should, so the average pressures remain high.

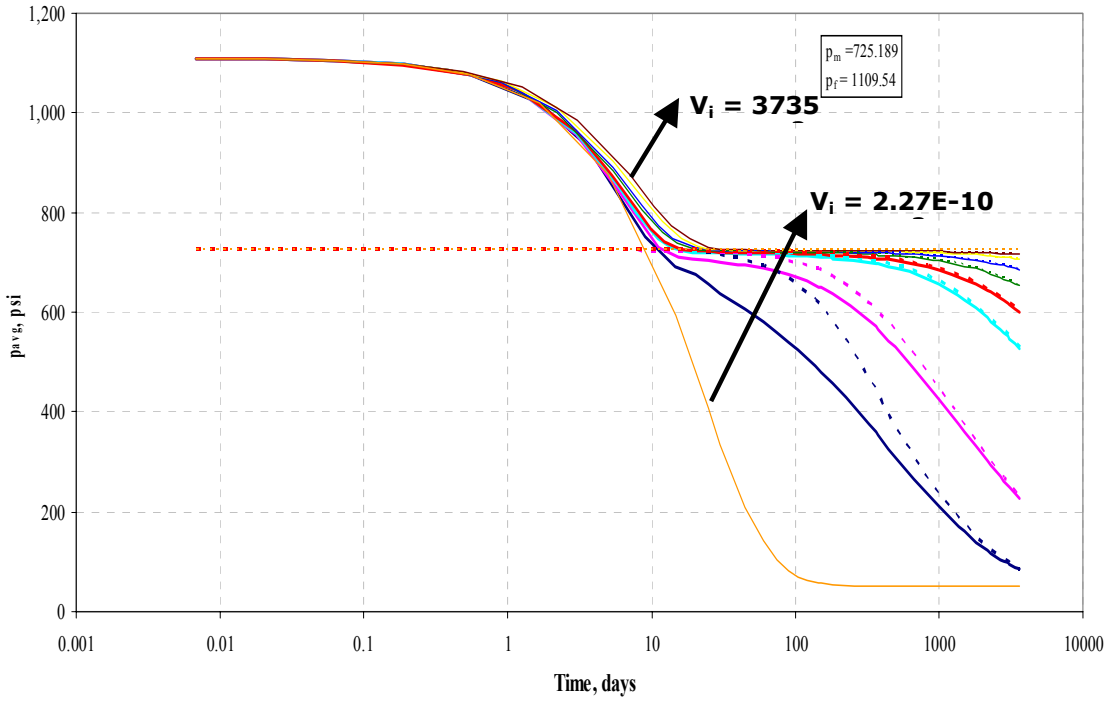

Figure D-1- Change in the matrix and fracture pressures with time for the varying cases of V_i ranging from 2.27E-10 scf/ft^3 to 3735 scf/ft^3.

VITA

NAME: Amarachukwu Ngozi Okeke

PERMANENT ADDRESS: 1222 Berrystone trail
Missouri City, Texas.
TX-77459

EDUCATION: B.Eng., Petroleum Engineering
Federal University of Technology, Owerri. Nigeria.
Dec 2000

M.S., Petroleum Engineering
Texas A&M University, August 2005